Recent Advances in Radiative Transfer Modeling and Microwave Land Surface Property Characterization

Jean-Luc Moncet
Atmospheric and Environmental Research, Inc.

Collaborators

- OSS
  - G. Uymin, A. Lipton
- LBLRTM/MonoRTM
  - V. Payne, E. Mlawer, J. Delamere
- Aura/TES retrievals
  - M. Shephard, K. Cady-Pereira
- Land surface
  - P. Liang, A. Lipton, J. Galantowicz, C. Prigent*
- Cloud 1DVAR
  - A. Lipton, R. d'Entremont, G. Gustafson

* LERMA (France)

Topics

- OSS review and status
- Multi-channel (global) training
- Radiance compression for retrieval/assimilation
- Spectroscopy improvements (MonoRTM/LBLRTM)
- MW Land surface property characterization
- Application to cloud property retrieval from imagers (MODIS)

OSS Review and Status

Review of the Basic OSS Method

- OSS channel transmittances/radiances modeled as weighted average of monochromatic transmittances/radiances (e.g. Moncet et al. 2001, 2003, 2008):

$$\overline{X} = \int_{\Delta\nu} \phi(\nu) X(\nu) d\nu \cong \sum_{i=1}^{N} w_i X(\nu_i); \qquad \nu_i \in \Delta\nu$$

- Wavenumbers ν_i (nodes) and weights w_i are optimally selected to fit calculations from a reference line-by-line model for a globally representative set of profiles (training set)

Relationship between OSS and ESFT/correlated-*k* methods

ESFT (Wiscombe and Evans, 1977) for single layer, single absorber case:

$$\bar{\tau}(u) = \int_{\Delta\nu} e^{-k_\nu u} d\nu \approx \sum w_i e^{-k_i u}$$

Extension to multiple absorbers along inhomogeneous path (e.g. Armbruster and Fisher, 1996)

$$\bar{\tau}(p) = \int_{\Delta\nu} \tau_\nu(p) d\nu \approx \sum w_i e^{-\sum_l \sum_m k_i^m(P_l,T_l) u_l^m}$$

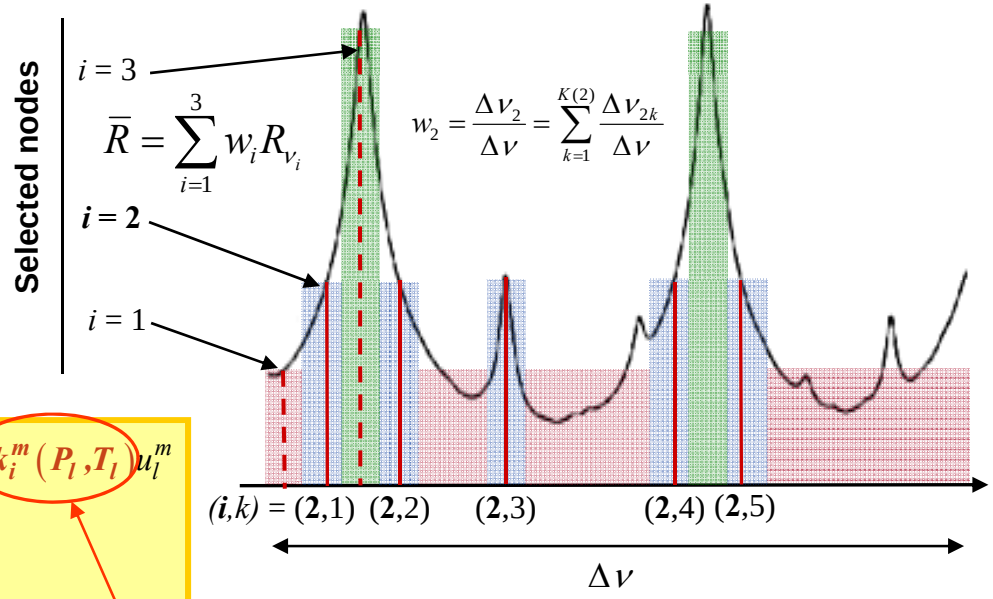

OSS solution:

$$\bar{\tau}(p) \approx \sum w_i e^{-\sum_l \sum_m k_{\nu_i}^m(P_l,T_l) u_l}$$

Extension of ESFT to inhomogeneous atmospheres with multiple absorbers reduces the problem to a single (wavenumber) dimension and ensures that the solution is physical

Training considerations

- Like TPTR methods (e.g. RTTOV, OPTRAN), necessitates line-by-line calculations for a set of globally representative profiles (training set)
- Search method for single channel (localized) approach is described in details in Moncet et al. 2008
  - Idea is to add nodes (chosen among initial set of monochromatic frequencies generated by lbl model) sequentially until differences between reference line-by-line calculations and OSS model are below some user-defined threshold
  - Weights recomputed for each new candidate by linear regression
- Radiance training preferred for modeling a specific instrument
  - Radiance training naturally puts more emphasis (weight) on layers that contribute most to outgoing radiances.
  - Takes smoothly varying spectral functions (Planck, surface emissivity and cloud properties) into account
- Transmittance training used
  - for generic multi-purpose band models (e.g. MODTRAN, ONERA/MATISSE) – instrument function, viewing geometry not known in advance
  - As pre-processing step for speeding up training in scattering environments (e.g. UV/VIS instruments, limb scattering)

OSS forward model

- RTM structure
  - Main loop is the node loop
  - Monochromatic RT
  - Inner channel loop to update channel radiances and Jacobians
- Uses LUT of absorption coefficients for fixed and variable gases (specified on a node-by-node basis) given as a function of pressure and temperature
  - Self-broadening included for water vapor
  - Computation of $\partial \tau_l^0 / \partial u_l^m$ inexpensive

Pressure and temperature entries for 101-level model

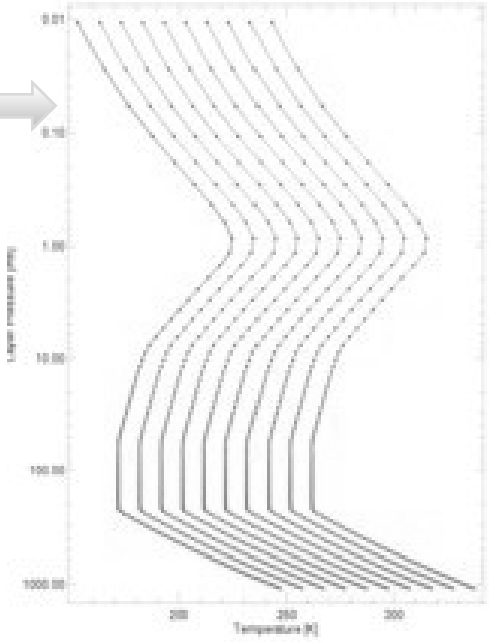

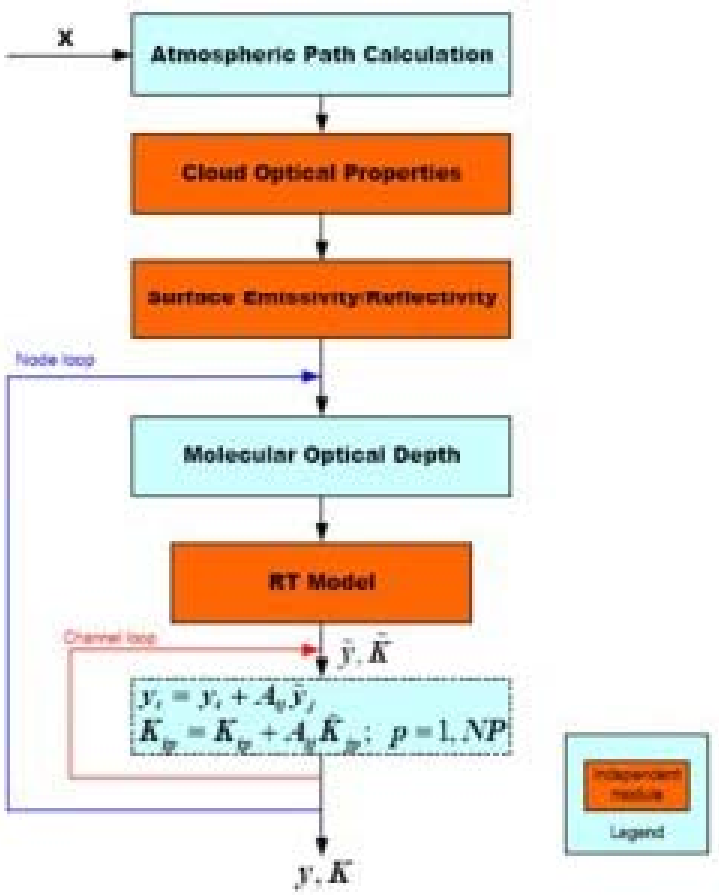

Profile data sources

1	H_2O	ECMWF with noise added; same as standard training set
2	O_3	ECMWF with noise added; same as standard training set
3	CO_2	GMI ±10°lat, ±1 month match, plus 2002-2012 secular trend, noise added on primary and secondary levels and interpolated
4	CH_4	GMI ±10°lat, ±1 month match, plus 2002-2012 secular trend, noise added on primary and secondary levels and interpolated
5	N_2O	GMI ±10°lat, ±1 month match, noise added on primary and secondary levels and interpolated
6	CO	GMI ±10°lat, ±1 month match, noise added on primary and secondary levels and interpolated
7	F11	GMI ±10°lat, ±1 month match, noise added on primary and secondary levels and interpolated
8	F12	single profile from Matricardi w/ ±10% random scaling
9	CCl_4	single profile from Matricardi w/ ±10% random scaling
10	HNO_3	single profile from Matricardi scaled to get 0.4 DU, then randomly varied by ln(q')=ln(q)±ln(5) (varied by factor of 5)
11	SO_2	single US Standard Atmosphere profile scaled to get 0.1 DU, then randomly scaled (on a log scale) to get random range of 0.09 to 900 DU. The scale factor is a two-piece hyperbolas of log(p), with the maximum factor D (and zero vertical derivative) at 235 mb tapering to D/1000 at the top and D/100 at the bottom. The rate of tapering was arbitrary.
12	OCS	constant with height at 500 pptv from surface up to 20 km an then linearly decrease to 0 at 50 km; the suggested dynamic range (randomized) is ±10% (per S. Tjemkes)
13	CF_4	dynamic range (randomized) of 50 to 70 pptv, constant profile (per S. Tjemkes)
14	NH_3	Derived from profiles over Australian fires and sugar cane fields provided by Guergana Guerova, University of Wollongong
15	HCOOH	ATMOS profile
16	CH_3OH	GEOS-CHEM profile provided by Dylan Millet. Harvard University
17	C_2H_2	Remedios [MIPAS team]: mean profile and 1-STD variability. For the training we use N-STD
18	C_2H_4	ATMOS profile
19	HCN	Remedios [MIPAS team]: mean profile and 1-STD variability. For the training we use N-STD
20	$CHClF_2$ (F22)	Remedios [MIPAS team]: mean profile and 1-STD variability. For the training we use N-STD

4 fixed gases (source AFGL standard atmospheres):
O_2, NO, NO_2, N_2

Number of variable trace species can be decided at run time. Non-selected species are assigned user-supplied profile and merged with fixed gases (no retraining required)

**Newly added variable species for Aura-TES

Trace gases

Where trace gases are active

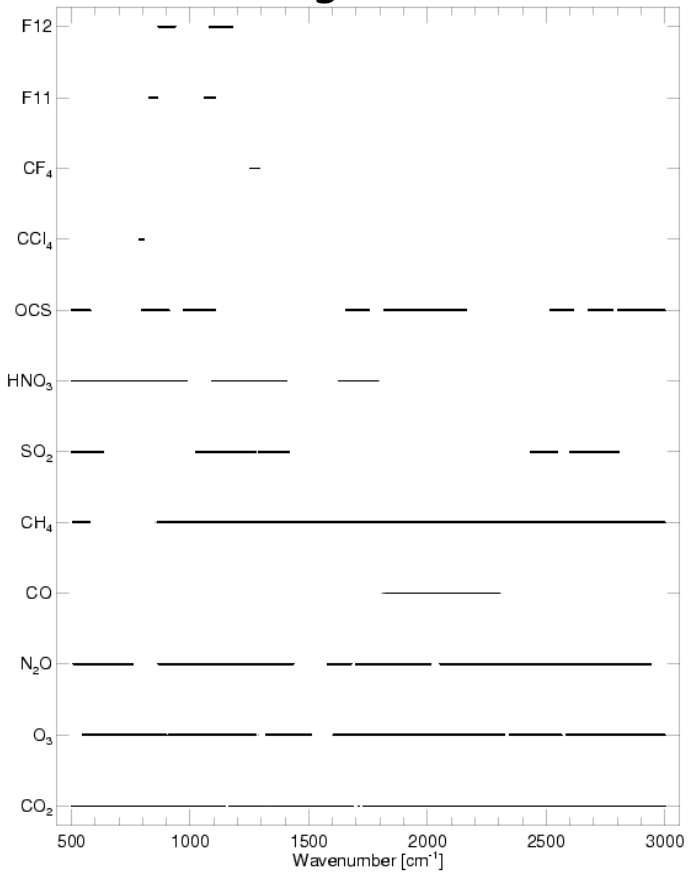

IASI results

Number of gas species active

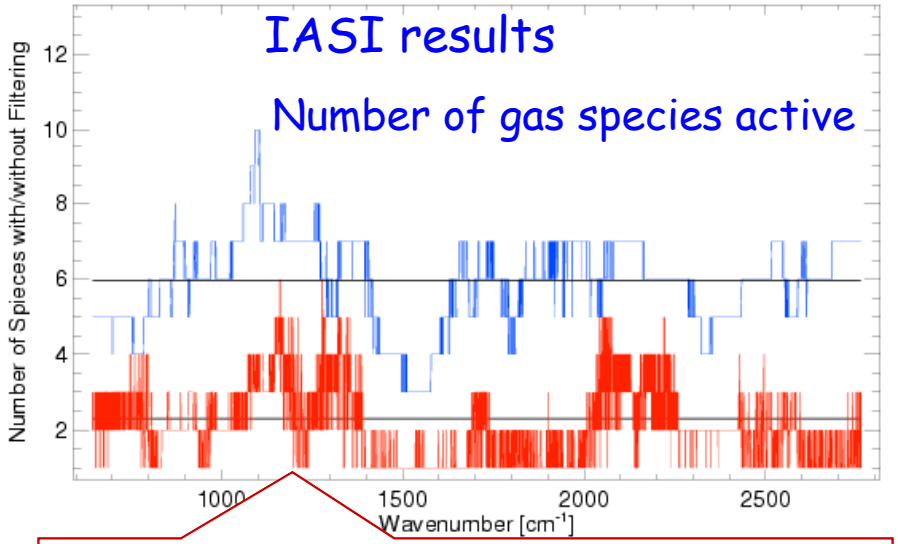

After filtering to retain only the species that significantly affect optical depth

# of variable species	Filter	Avg. # of species /node	Timing (s)	
			Fwd only	Fwd+ Jacobians
2	No	1.89	0.20s	0.36s
	Yes	1.31	0.18s	0.28s
13	No	5.97	0.29s	0.67s
	Yes	2.30	0.22s	0.39s

Timing not much affected by adding species

AIRS Application

Local training results

AIRS (2378 channels):

- Average: 11 nodes weighted per channel
- Average: 1.3 nodes/channel overall (accounts for sharing)

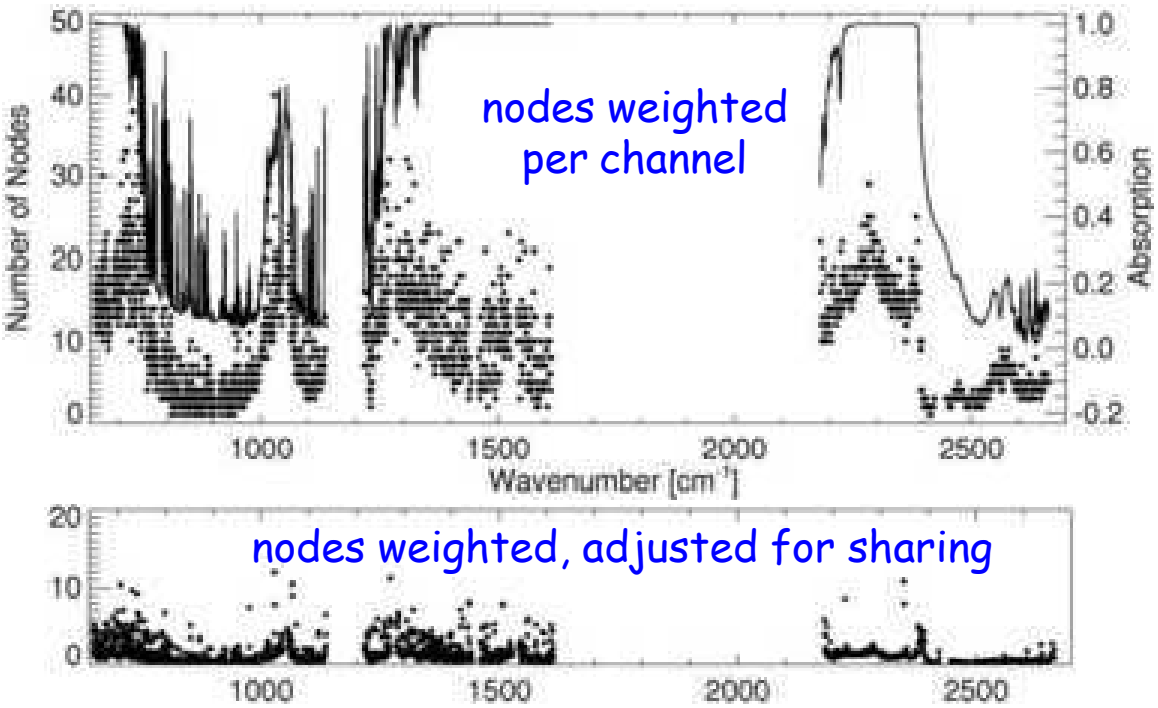

for this case, only variable gases were H_2O and O_3

OPTRAN/OSS comparisons for AIRS Channels (by NOAA, 2005)

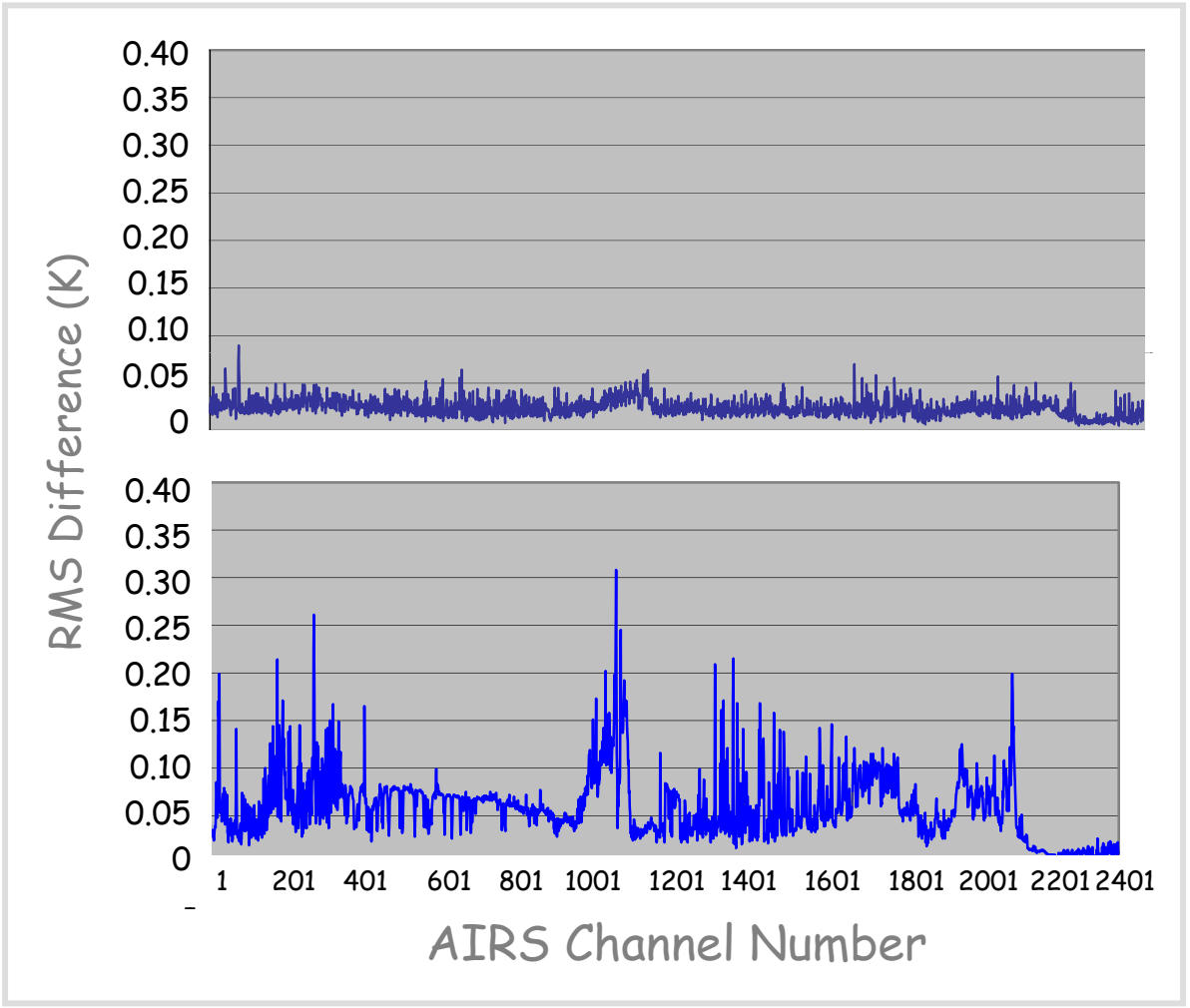

OSS
Trained with ECMWF set (local training)
Tested with UMBC set
(Training accuracy = 0.05K)

OPTRAN
Trained with UMBC set
Tested with ECMWF set

OSS (local training) is ~ 1 order of magnitude faster than OPTRAN for full AIRS channel set

Application to IASI (from Tjemkes et al., 2008)

- OSS selected by EUMETSAT for the MTG-IRS L2 concept processor development
- Among candidate FRTMs for MTG operational ground segment
- OSS and RTIASI provide similar accuracy (limited by knowledge of spectroscopy) when compared to real IASI data
- OSS significantly faster than RTIASI

FRTM	Only Radiance	Radiance and Jacobians
RTIASI	1.12	11.42
OSS	...	0.78

Table 1 The average time in sec. to process one profile by RTIASI and OSS on a IBM power 4.

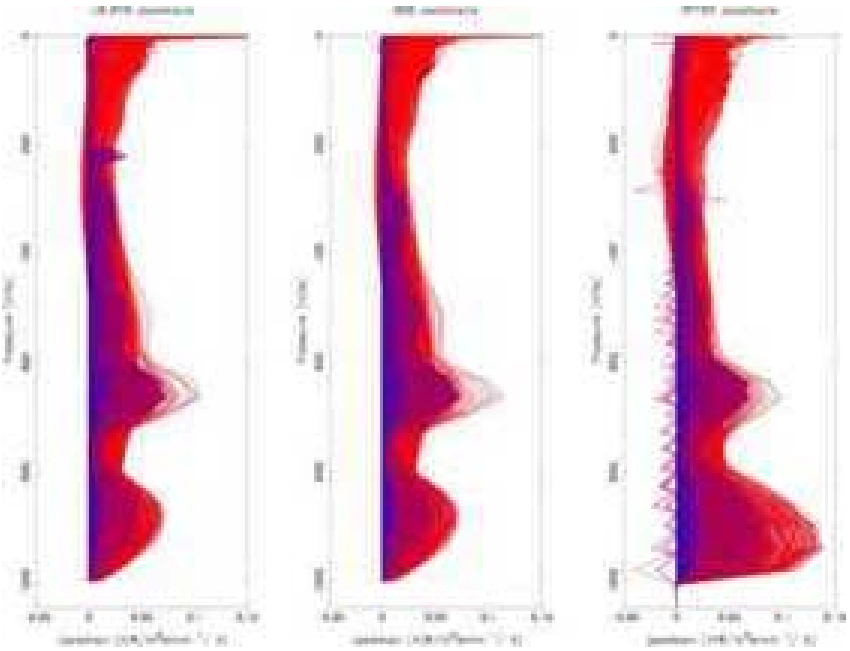

Temperature Jacobians for all IASI channels obtained for single atmospheric profile with LBLRTM, OSS and RTIASI*. Wavenumber increases from blue to red.

Good overall agreement between temperature and moisture Jacobians generated by LBLRTM, OSS and RTIASI. Near the surface, RTIASI Jacobians appear to be stronger.

* Negative spikes in the RTIASI temperature jacobians are the results of the particular coefficient file used. New file prepared by M. Matricardi removes the spikes

Application to IASI (from Tjemkes et al., 2008)

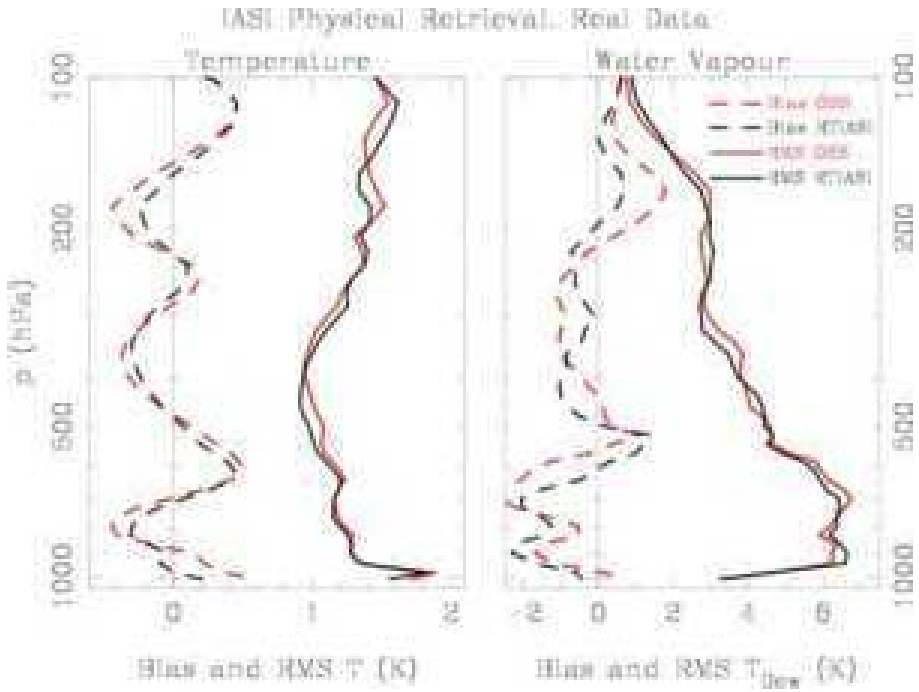

Exp	EOF	OE	Retrieval	RTM module
Baseline	RTIASI	RTIASI	502	246.3
Alternative	OSS	OSS	269	10.0

Table 2 Setup and timing results of entire retrieval and the RTM module alone (for one non-lineair retrieval in sec) of the 2 retrieval Experiments.

Summary of Retrieval Experiments

- *Moisture and Temperature retrievals based upon OSS* have similar rms compared to similar retrievals based upon RTIASI.
- *Retrievals are more efficient using OSS than RTIASI.*

Multi-channel (global) training

Concept

- OSS formalism (described previously for single channel) can conceptually be extended to problem of minimizing model errors in many channels simultaneously
- Goal: minimize total number nodes (Ntot) needed to represent an entire band (at the cost of increasing the number of nodes - Nav - used to describe any single channel within the group).
- Direct application of single channel formalism to multiple channels not feasible in practice: initial set of candidates nodes (and average number of nodes needed to represent a single channel) too large!
- Current approach: use radiance clustering to exploit inter-nodal correlations to reduce up front number of candidate nodes

Methodology trade

- Two approaches considered:
- Method 1: Reduce initial number of nodes by clustering below minimum required to model the spectral domain and add back nodes on a channel per channel basis until all channels meet accuracy threshold.
- Method 2: Apply clustering to reduce initial number of nodes to N > Nmin. Apply extended (vector) search for final selection.
- Look for fastest implementation and capability of providing continuous trade off between minimizing Nav (local training) and Ntot (global training).

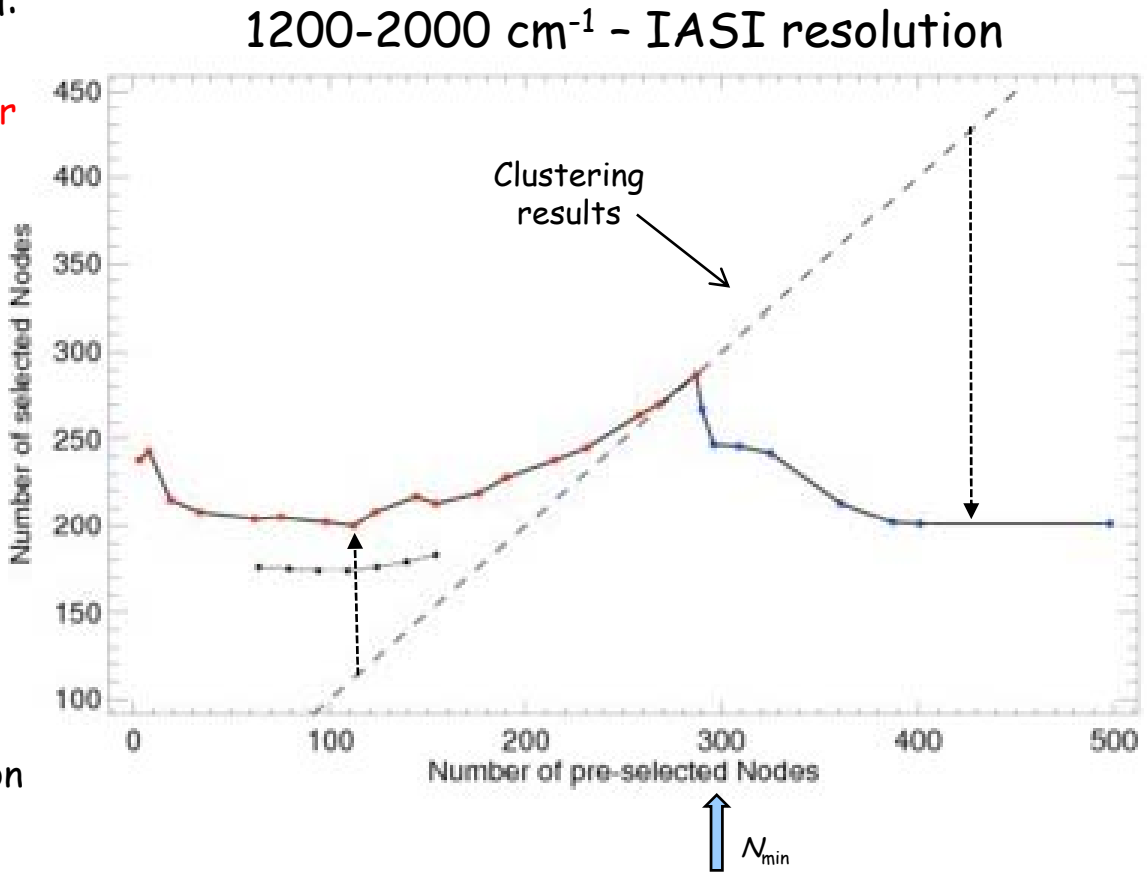

Handling of clouds

- When working over extended spectral domains, need to take into consideration variations in cloud optical properties (as well as surface emissivity and Planck function across the domain)
- It has been shown that OSS nodes and weights act as spectral interpolators for the smooth spectral functions
- Training strategy: train with clear and cloudy radiance sets and simultaneously minimize modeling errors in the two sets

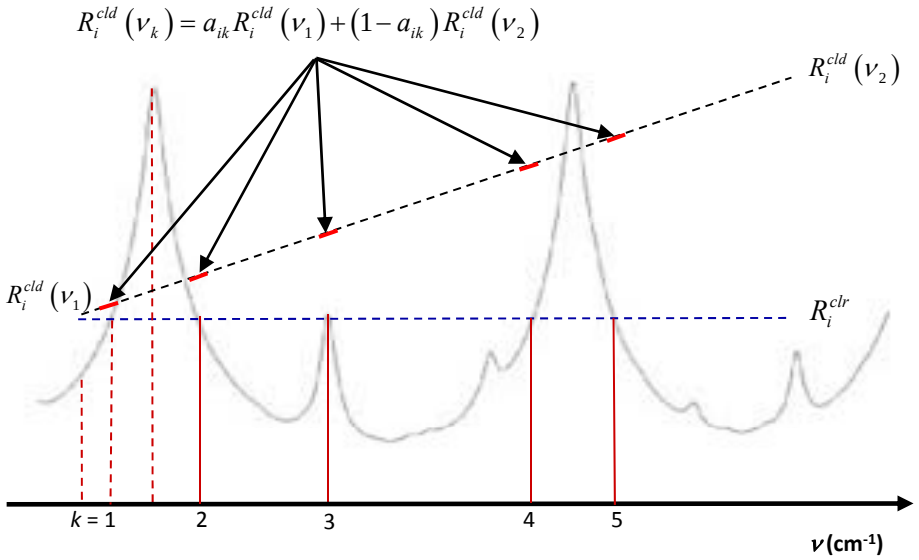

Application to IASI

Global and local training results

IASI band	Spectral range (cm^{-1})	Number of channels	Number of nodes: Local	Number of nodes: Global	Global nodes/ channels
1	645-1210	2261	1855	185	0.082
2	1210-2000	3160	2927	231	0.079
3	2000-2760	3040	2639	203	0.067
Total		8461	7421	619	

Global training reduces #nodes by ~order of magnitude

Training conditions:

- Accuracy < 0.05 K (all channels)
- 13 variable gases: H_2O, O_3, CO_2, CO, CH_4, N_2O, F11, F12, CCl_4, HNO_3, SO_2, OCS, CF_4
- 5 fixed gases: O_2, NO, NO_2, NH_3, N_2
- Sources: ECMWF for H_2O, O_3; Global Modeling Initiative chem model for CO_2, CO, CH_4, N_2O, F11, M. Matricardi for F12, CCl_4, HNO_3
- 2002-2012 secular trends added for CO_2 and CH_4
- Randomization was applied to all species for robust training
- Emissivity spectra for global training is random walk, with 20-cm^{-1} steps

Reduction in # of nodes translates in a factor ~10 speed up of the RT model, when not doing Jacobians
(w/ Jacobians, get speed up only if PC or node-based retrieval/assimilation is adopted)

Application to GOME

- Ocean – no clouds
- Variable gases: H2O, O3
- Aerosols Optical Thickness: 0-0.4
- Global training (accuracy: 0.25%)

	Band 2	Band 4
Spectral range	290-370nm	580-770nm
#Channels	910	828
# Nodes	22	44
Nav	3.47	3.36

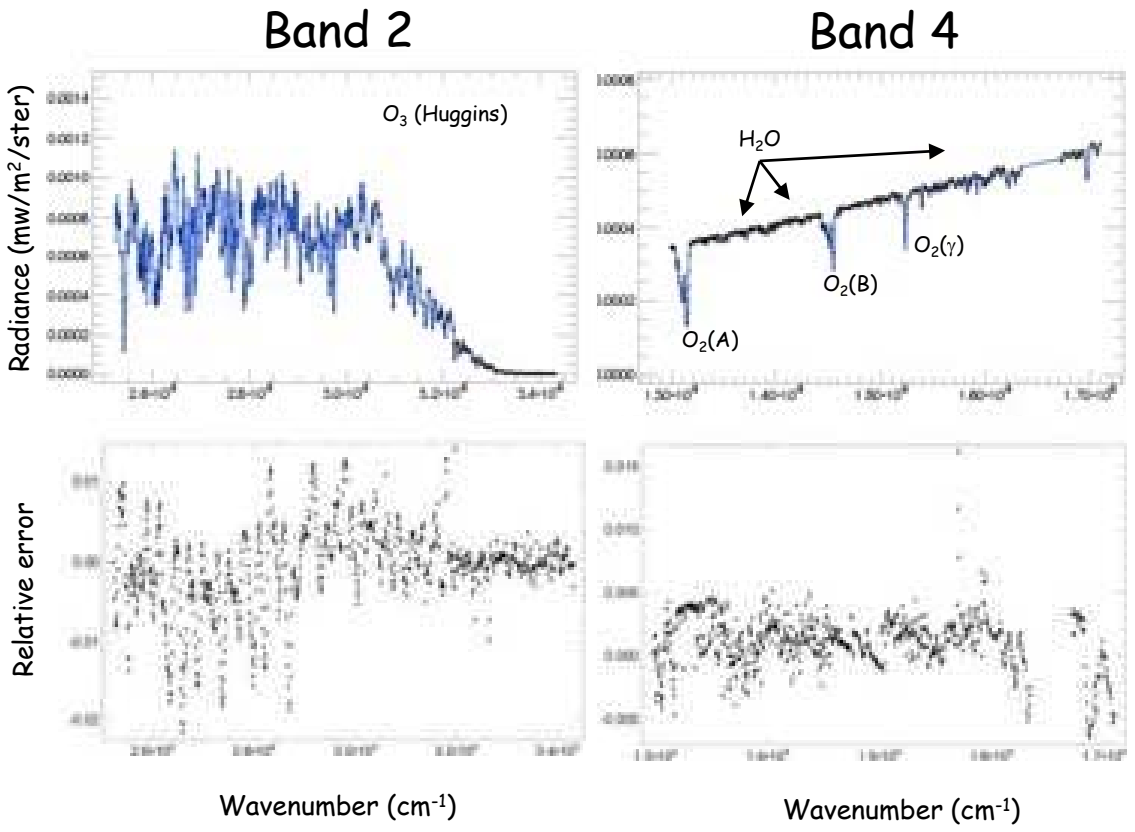

LOA (Univ. Lille)/GAME

OSS

High spectral resolution spectral radiance compression in retrieval/assimilation

OSS with Principal Components of Radiance Spectrum

- Variational retrieval/assimilation methods:
  - Average channel uses ~150 nodes
  - Mapping Jacobians from node to channel space partially offsets forward model speed gain
- PC option may be useful (for radiance compression and reducing algebra in inversion) when some information loss is accepted as trade-off for speed
  - When eigenvector truncation goes beyond eliminating redundancy
- Can be done without significant revision to OSS training
  1. Filter training-profile radiances with truncated eigenvectors
     - Convert to PCs, then use reverse transformation to recover channel radiances
  2. OSS radiance training achieves required accuracy for every channel (PC filtered)
  3. OSS coefficients project only on retained PCs (within training accuracy)
- Forward model output in terms of PCs efficiently done by combining eigenvectors with OSS coefficients in advance:

$$\mathbf{y} = \mathbf{A}\,\tilde{\mathbf{y}} \qquad \mathbf{PC} = \mathbf{U}_m\,\mathbf{y} \quad \text{with } m \text{ retained PCs}$$

$$\mathbf{PC} = \mathbf{U}_m\,\mathbf{A}\,\tilde{\mathbf{y}} = \mathbf{A}_m\,\tilde{\mathbf{y}} \qquad \text{where} \qquad \mathbf{U}_m\,\mathbf{A} \equiv \mathbf{A}_m$$

NH_3 and CH3OH spectral signatures in the TES observations over Beijing (Beer et al., 2008, JGR)

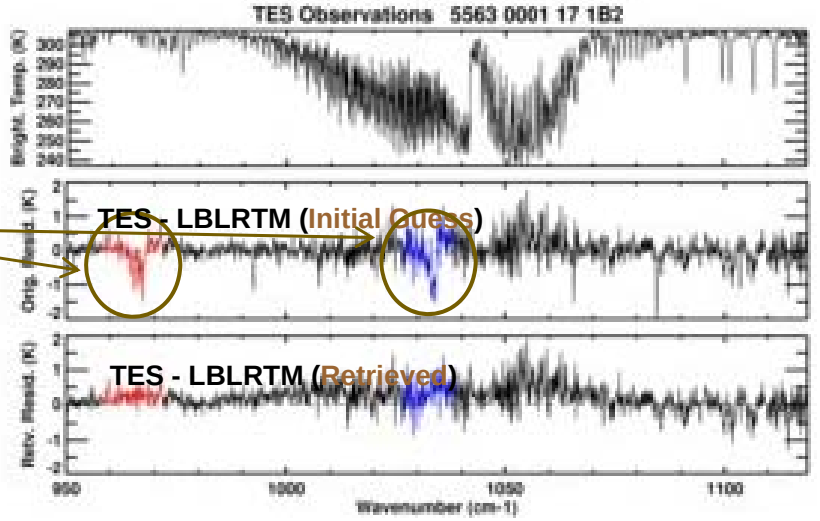

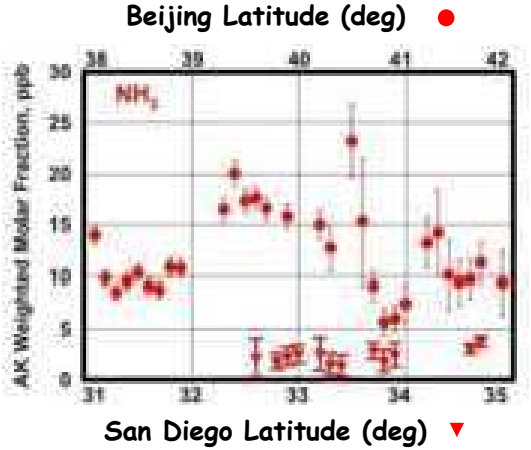

Retrieval/Assimilation in Node Space

- Exploring alternative to PC
  - Project observations in node space

    $\tilde{\mathbf{y}}_{obs} = \mathbf{H}\mathbf{y}_{obs}$ where $\mathbf{H} = \left(\mathbf{A}^{\mathrm{T}}\mathbf{S}_{\varepsilon}^{-1}\mathbf{A}\right)^{-1}\mathbf{A}^{\mathrm{T}}\mathbf{S}_{\varepsilon}^{-1}$

    (associated inverse error covariance matrix $\tilde{\mathbf{S}}_{\varepsilon}^{-1} = \mathbf{A}^{\mathrm{T}}\mathbf{S}_{\varepsilon}^{-1}\mathbf{A}$)
  - Perform retrieval in node space (mathematically equivalent to replacing observation vector $\mathbf{y}_{obs}$ by $\mathbf{AHy}_{obs}$ in original inversion equation)
  - Avoids Jacobian transformation from nodes to channels, and reduce K-matrix size (inversion speed up): for AIRS, 2378 channels -> ~250 nodes
  - Directly applicable to cloudy observations, minimum loss of information
  - When radiometric noise can be assumed independent of scene temperature, matrices $\tilde{\mathbf{S}}_{\varepsilon}^{-1}$ and $\mathbf{H}$ can be computed once off-line otherwise need strategy to avoid frequent updates

Example of AIRS retrieval performance

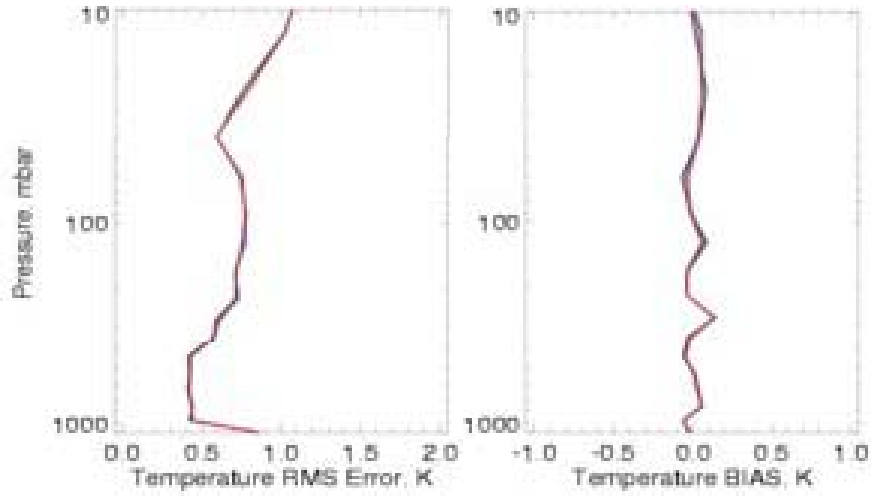

Spectroscopy Improvements (MonoRTM/LBLRTM)

Water vapor: Line widths

Payne et al., IEEE TGRS (2008)

22 GHz:
MonoRTM 5% lower than RK

183 GHz:
MonoRTM ~ same as RK

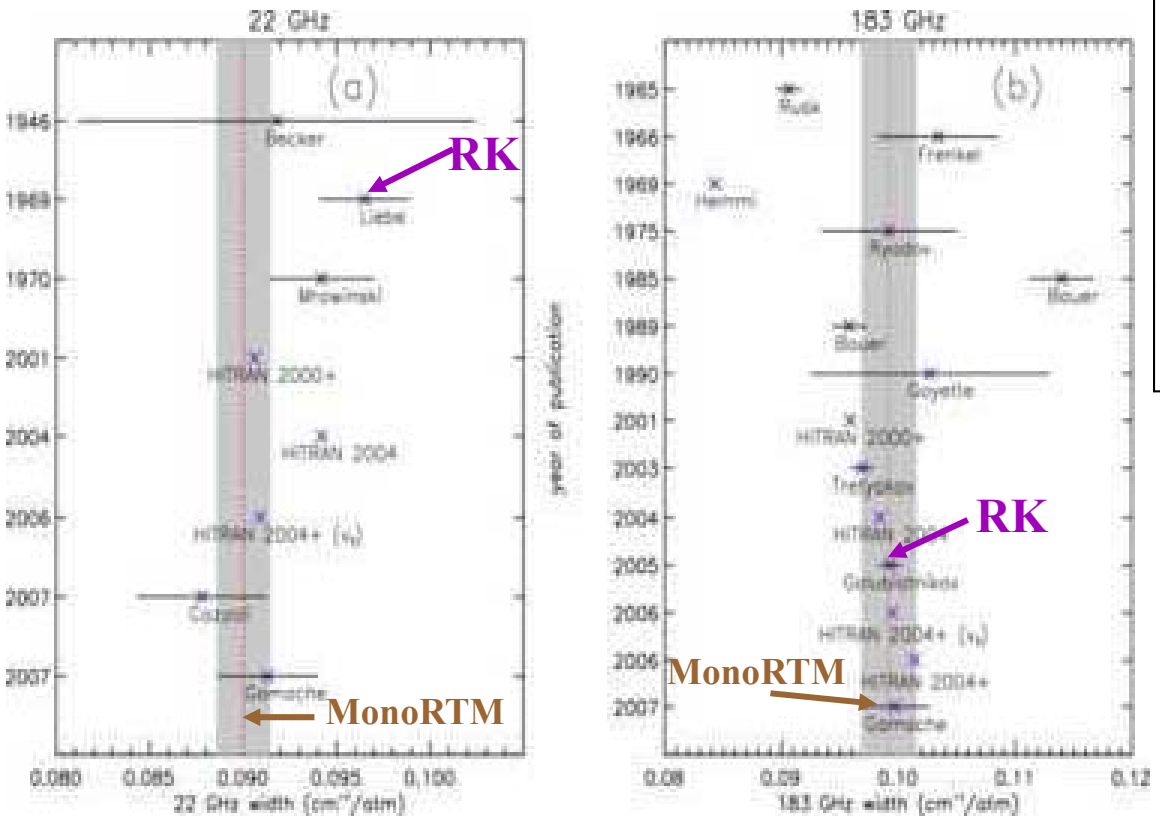

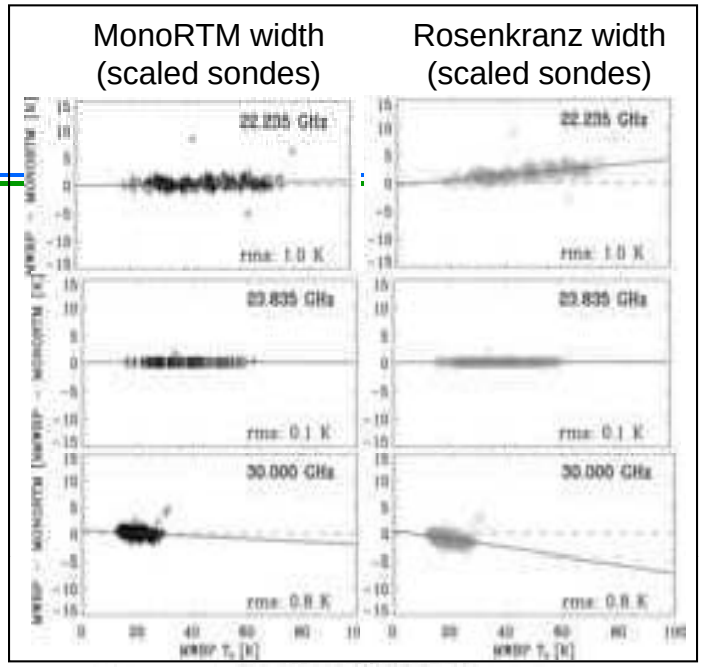

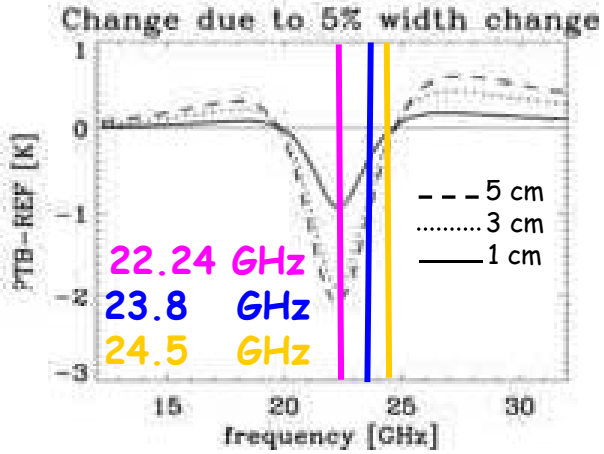

Incorrect specification of the 22 GHz width will lead to inconsistency between e.g. AMSU/AMSR-E and SSM/I -SSMIS

Additional evidence for lower 22GHz width value from upwelling radiation:

»UK Met Office (W. Bell and P. J. Rayer - lower width improves SSMI biases)

»Tom Wilheit (Texas A&M) - TMI and SSMI

Water vapor: Self and foreign continuum

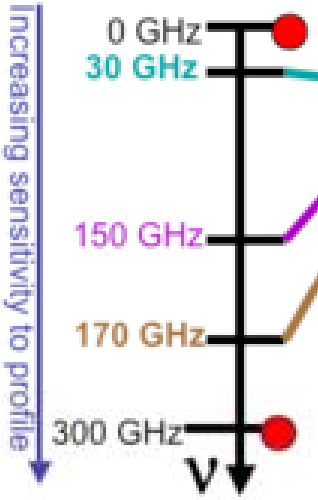

Instrument	Location	Dates	Max. PWV
MWR	SGP	1993-2008	5 cm
MWRHF	COPS (FKB)	06/07-01/08	3 cm
MP183	SGP	01/08-03/08	3 cm

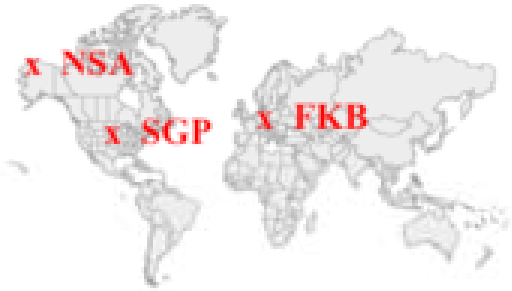

Retrieve PWV scaling factor using 23.8 GHz MWR channel.

Assess the quality of the fit in the "window" channel.

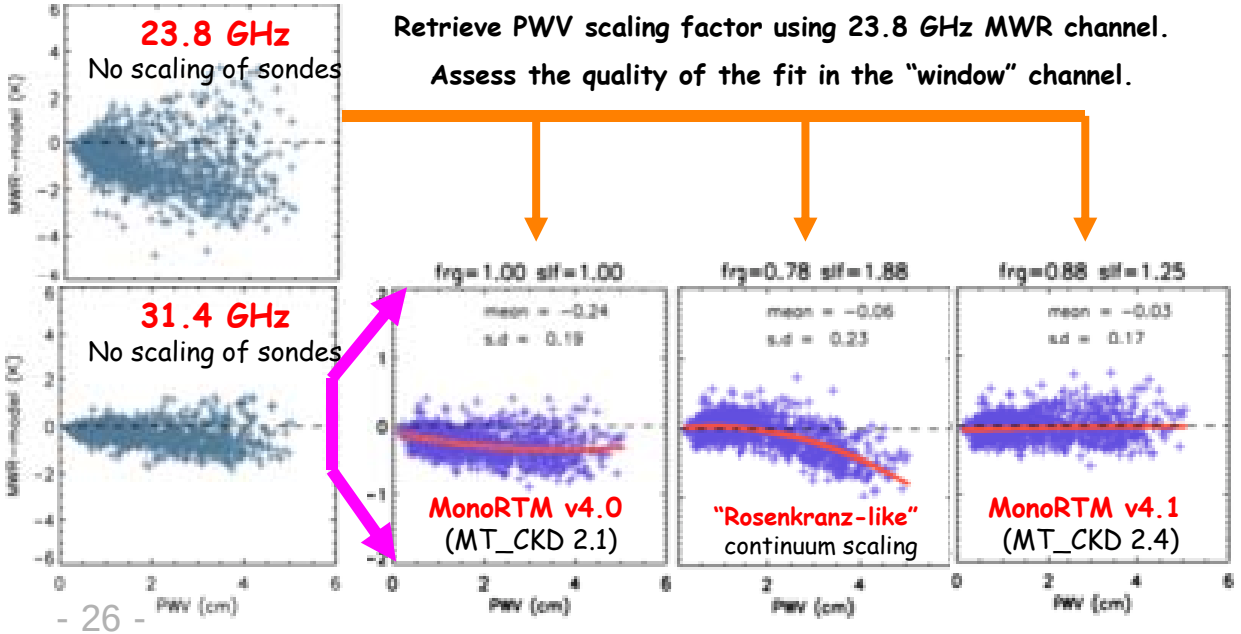

Cost function for window channels for different self and foreign continuum scaling combinations

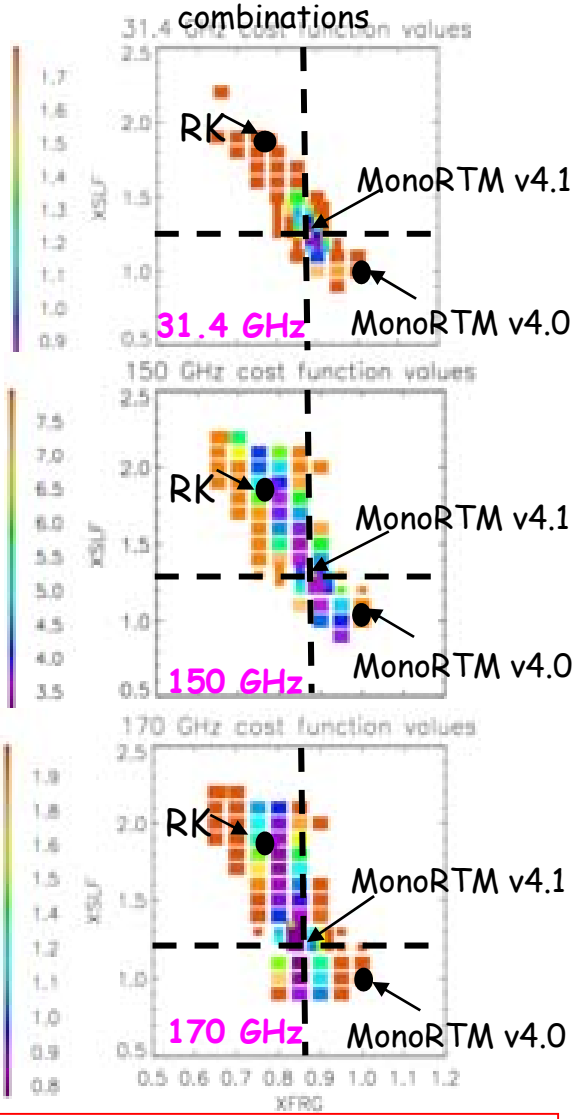

Consistent information from different instruments/frequencies!

Brightness temperature differences

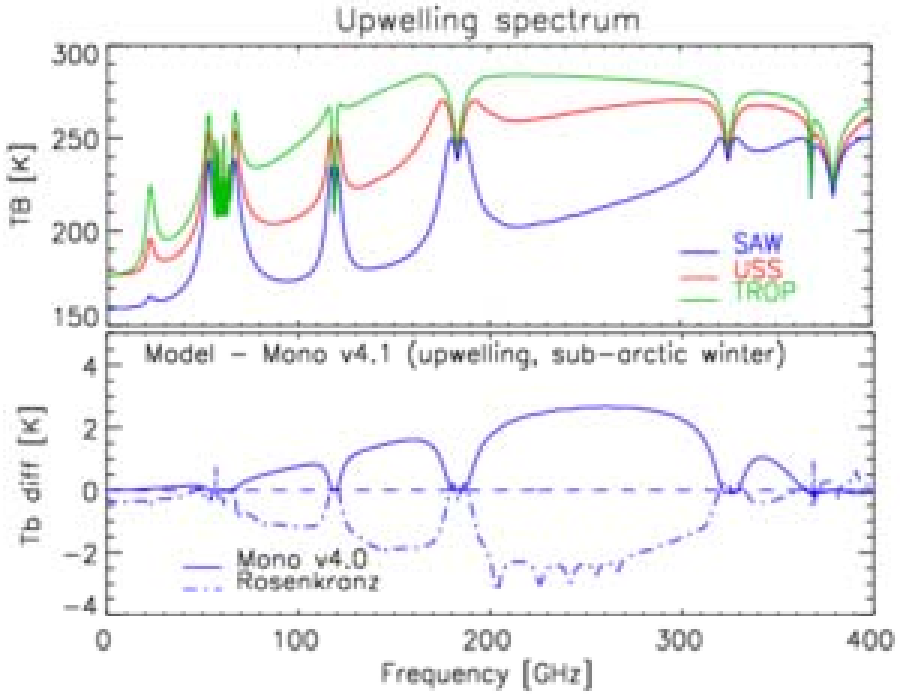

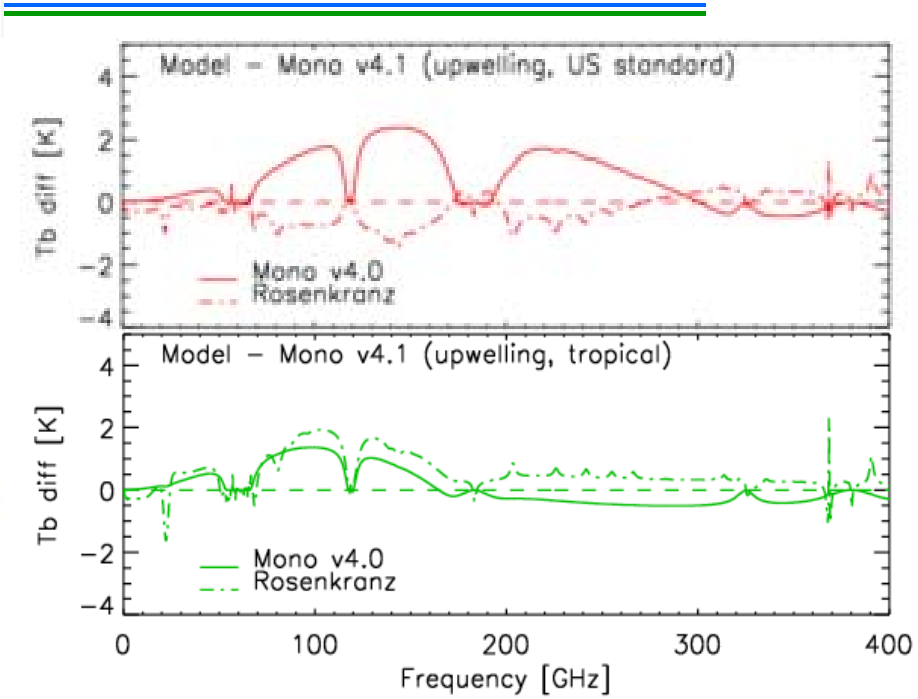

Note that RSS has recently readjusted their water vapor continuum to remove bias in CLW retrieval (Meissner and Wentz, *personal communication*). RSS and AER continua are now close together at 37 and 89 GHz (RSS model not valid above 89 GHz)

Consistency across Mid-infrared Spectral Regions

Mean residuals from 36 ARM TWP cases using Tobin et al. best estimate sonde profiles.

Profile inputs from AIRS Phase I val. supplied by L. Strow and S. Hannon (UMBC).

LBLRTM

CO_2 line coupling
Application of Niro et al. (2005)

H_2O line positions and strengths
Coudert et al. (2008)

CO_2 line positions and strengths
Tashkun et al., (1999)
Already in use by MIPAS team (Flaud et al., 2003)

H_2O shifts, T-dep. Of widths
Gamache (personal comm.)

CO_2/H_2O continuum
(see final LBLRTM v11.7 release)

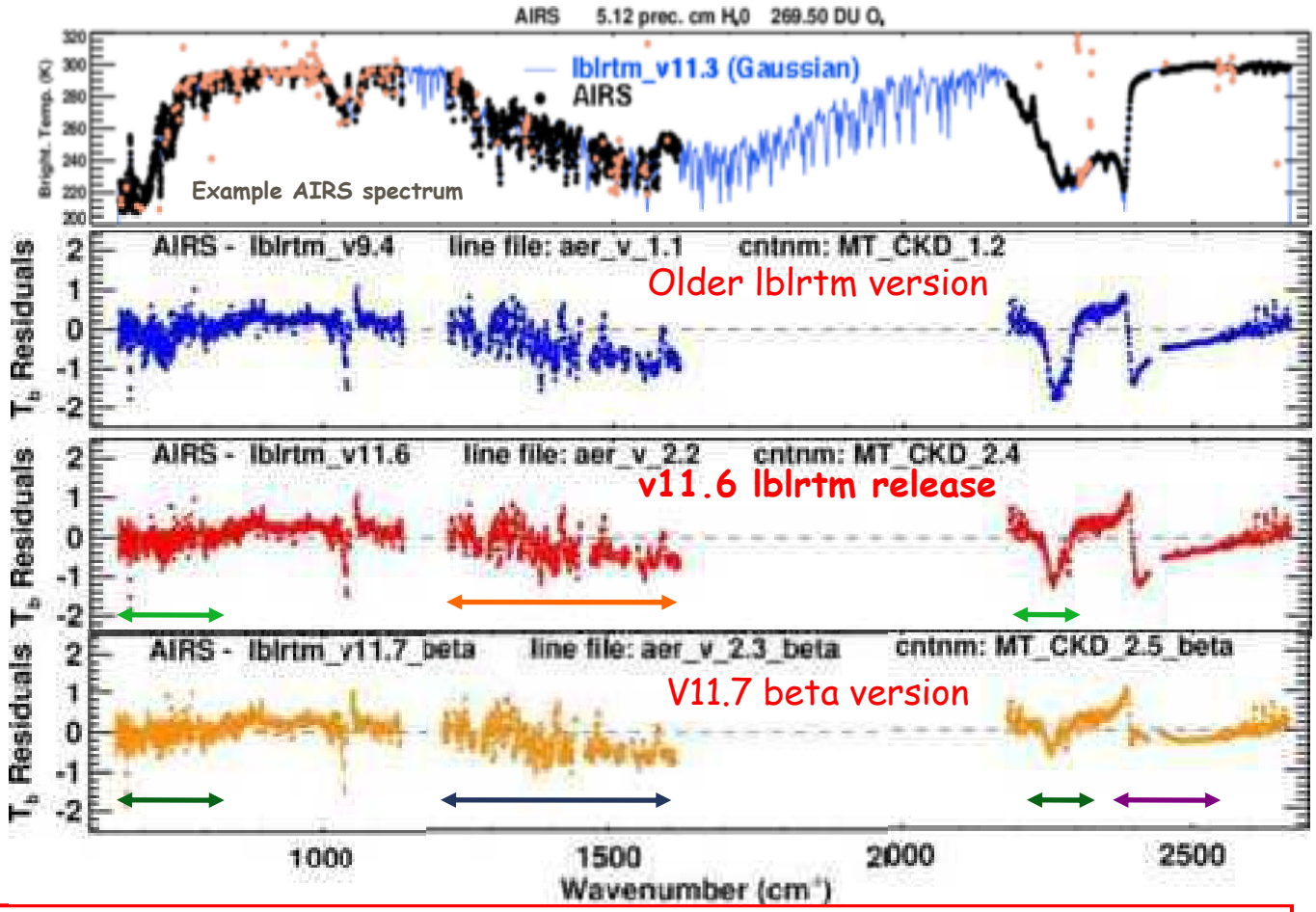

Significant improvements to consistency between spectral regions!

Carbon dioxide: consistency between ν2 and ν3 regions

Mean residuals from 36 AIRS ARM TWP cases using Tobin et al. best estimate sonde profiles
(Input profiles supplied by L. Strow and S. Hannon).

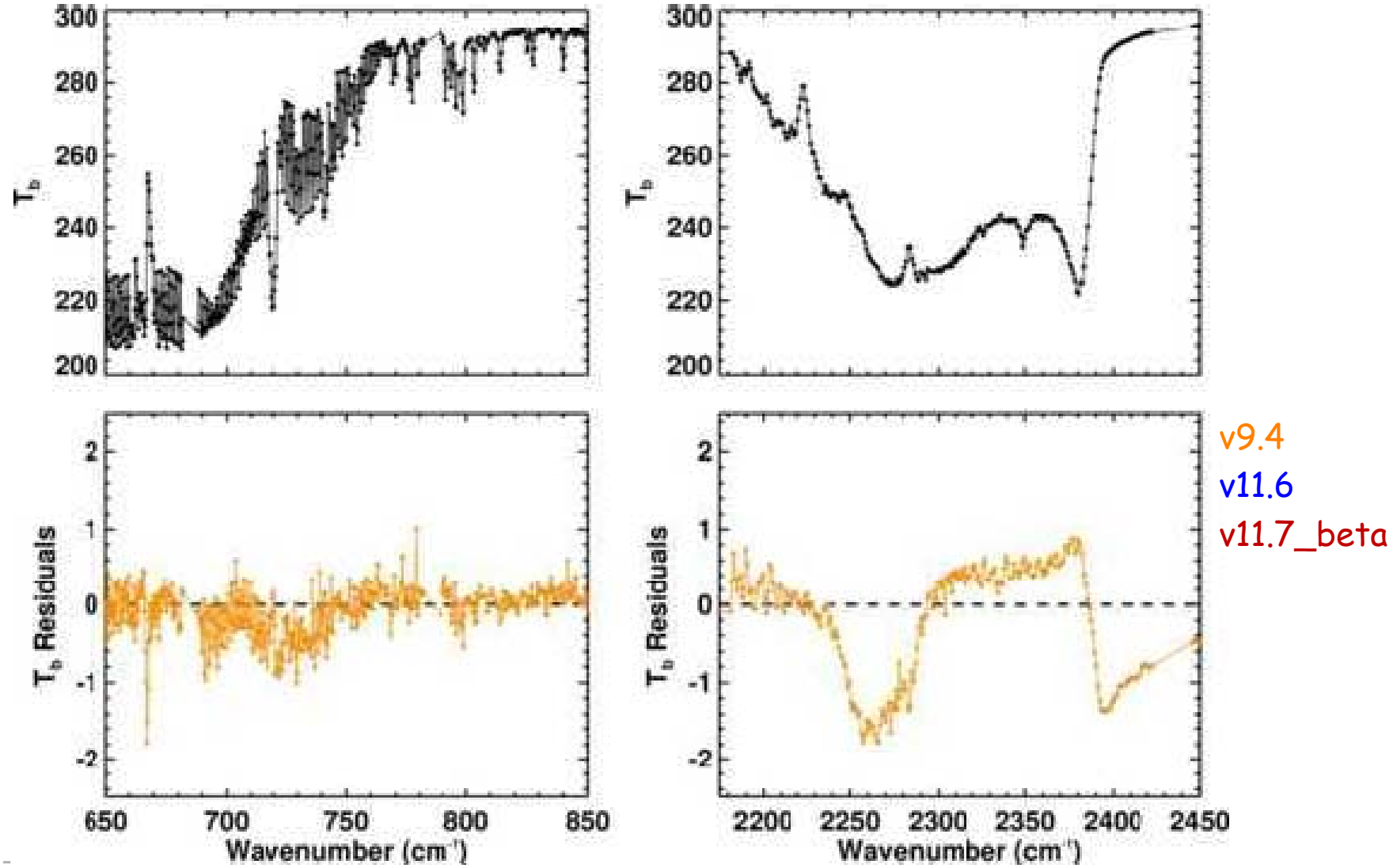

v9.4
v11.6
v11.7_beta

Carbon dioxide: consistency between ν2 and ν3 regions

Mean residuals from 36 AIRS ARM TWP cases using Tobin et al. best estimate sonde profiles
(Input profiles supplied by L. Strow and S. Hannon).

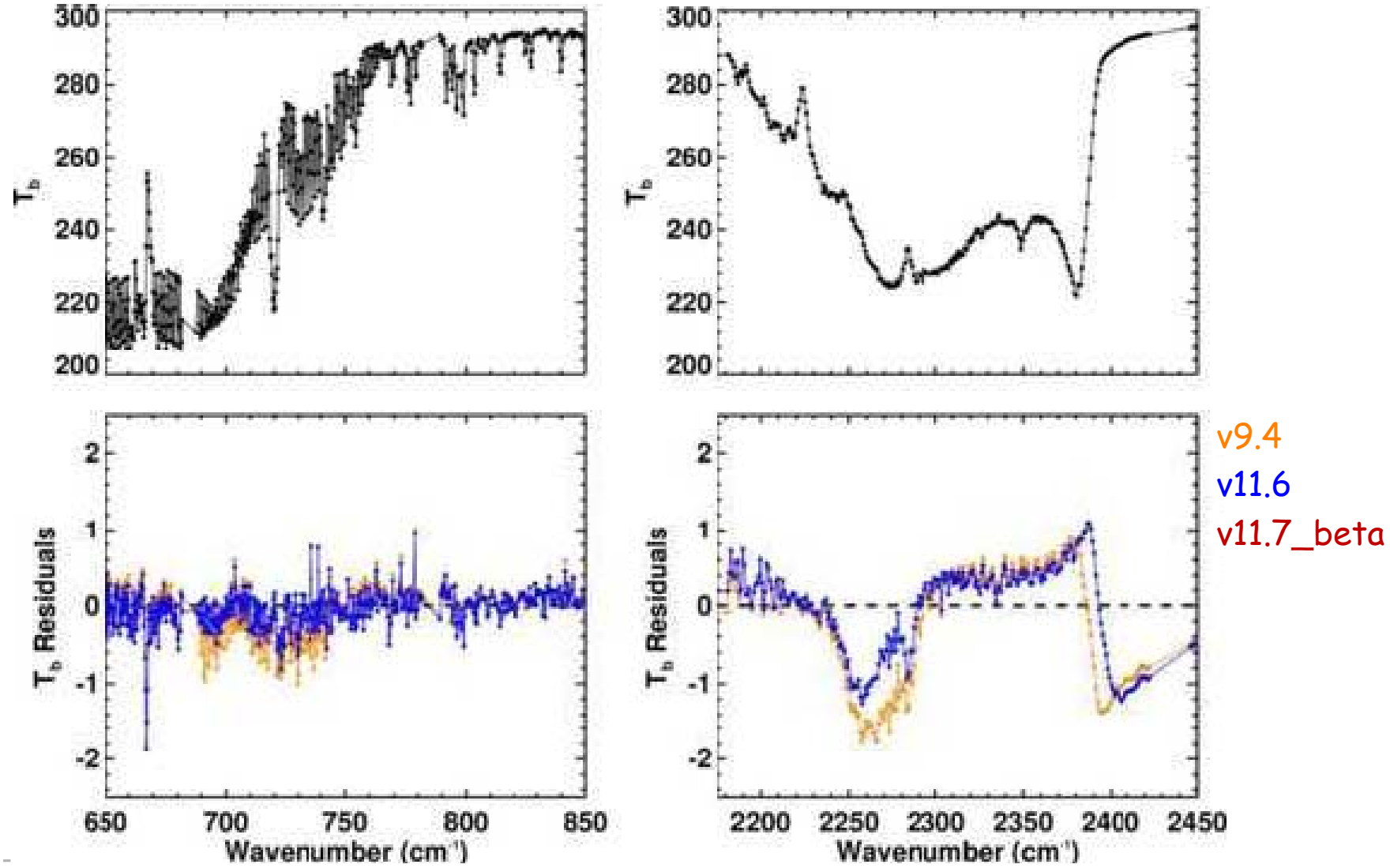

v9.4
v11.6
v11.7_beta

Carbon dioxide: consistency between ν2 and ν3 regions

Mean residuals from 36 AIRS ARM TWP cases using Tobin et al. best estimate sonde profiles
(Input profiles supplied by L. Strow and S. Hannon).

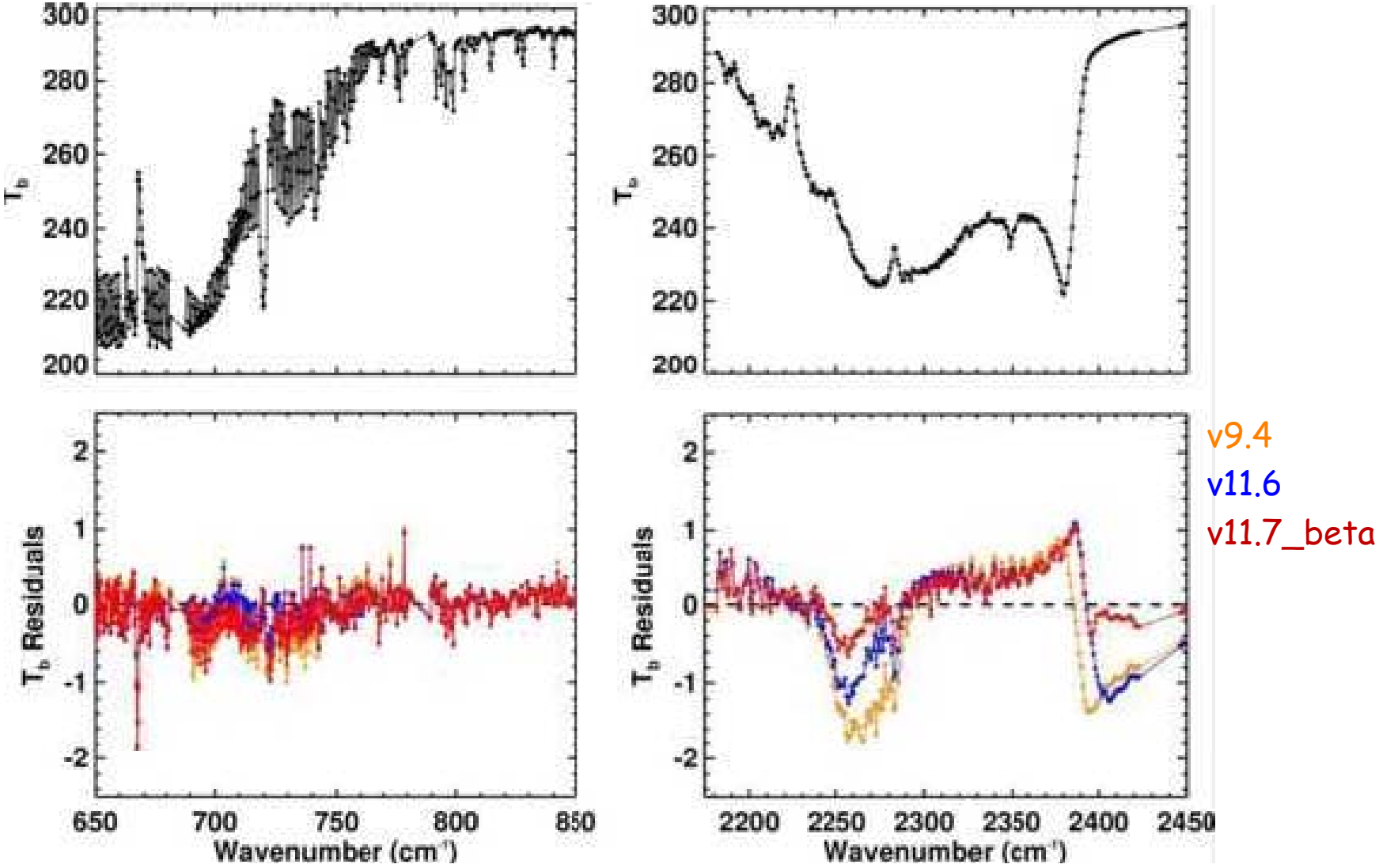

v9.4
v11.6
v11.7_beta

Water Vapor ν_2 Region : Impact of Coudert Intensities

IASI measurement from JAIVEx campaign

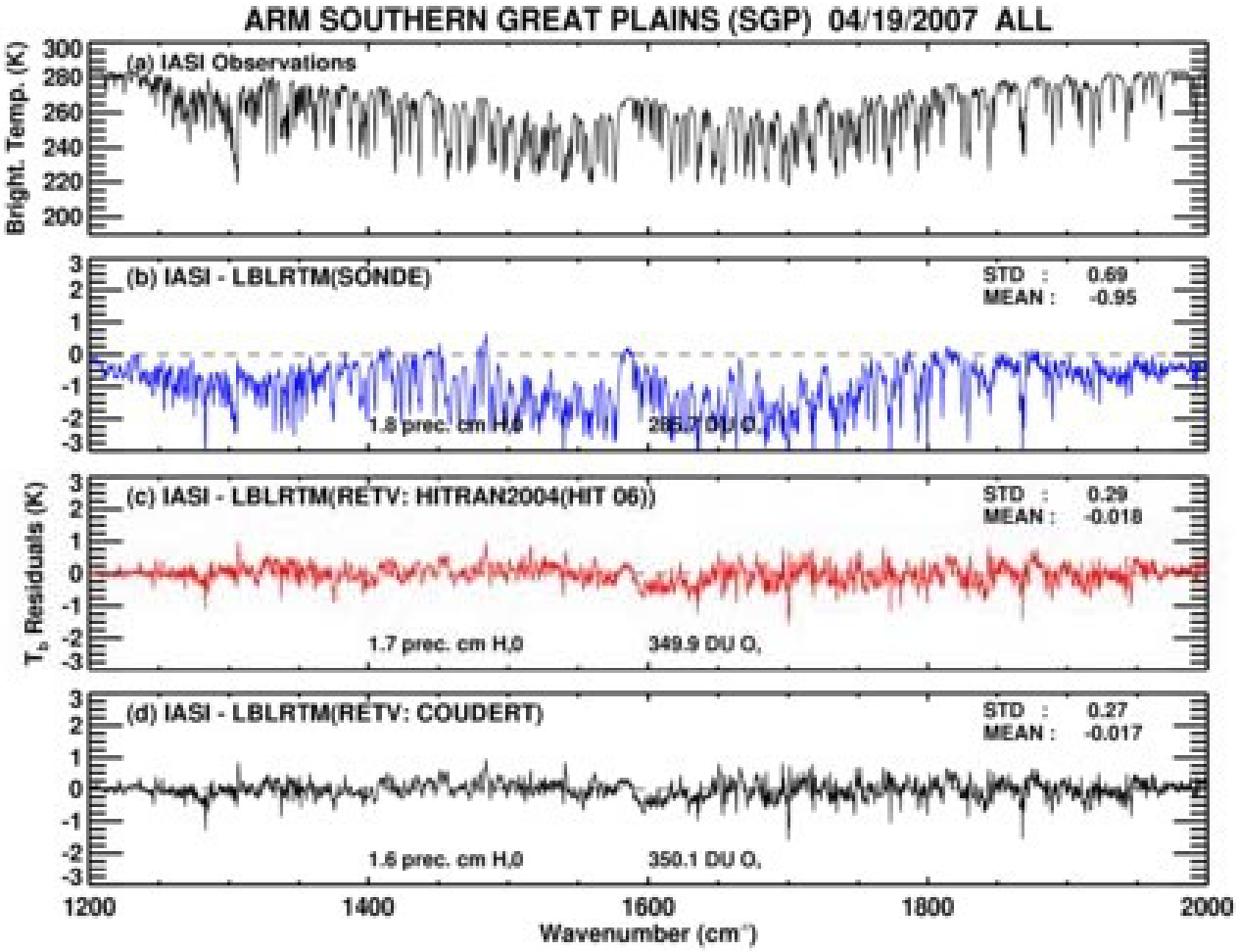

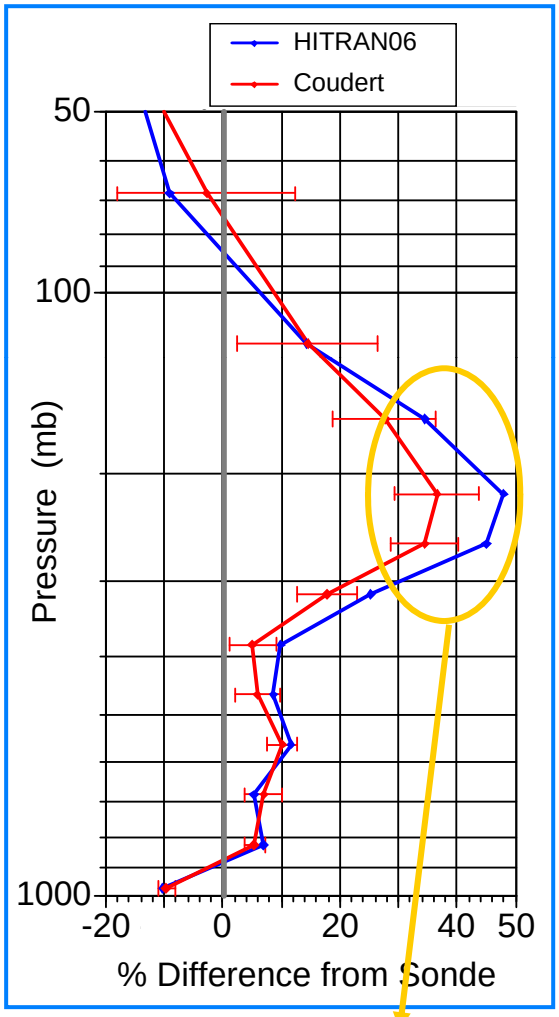

~10 % diff in upper troposphere

Tony Clough and Mark Shephard (Shephard et al., ACP, 2009)

$\nu 3$-CO_2 band head (v11.7 release)

- CO_2 continuum scaled to improve agreement with IASI observations in dry conditions (PW < 0.65 cm)
- Both IASI and AERI comparisons show significant dependence of residuals on temperature/water vapor (after CO_2 continuum adjustment):
  - Introduction of temperature dependence of CO_2 continuum based on line coupling coefficients at 200K, 250K and 340K in addition to 296K improves residual around 2395 cm^{-1}
  - Scaling of H_2O self broadened continuum by a factor up to 5-7 (consistent with laboratory measurements from Bicknell et al., 2006 and Fulghum and Tilleman, 1991 in the near IR) in 2000-3000 cm^{-1} region improves fit in window region

V11.7 - IASI comparisons

- No sonde temperature profile correction (based on retrieval using 15 μm band – future work)
- Positive impact of modifications on comparisons with AERI and AIRS (control).

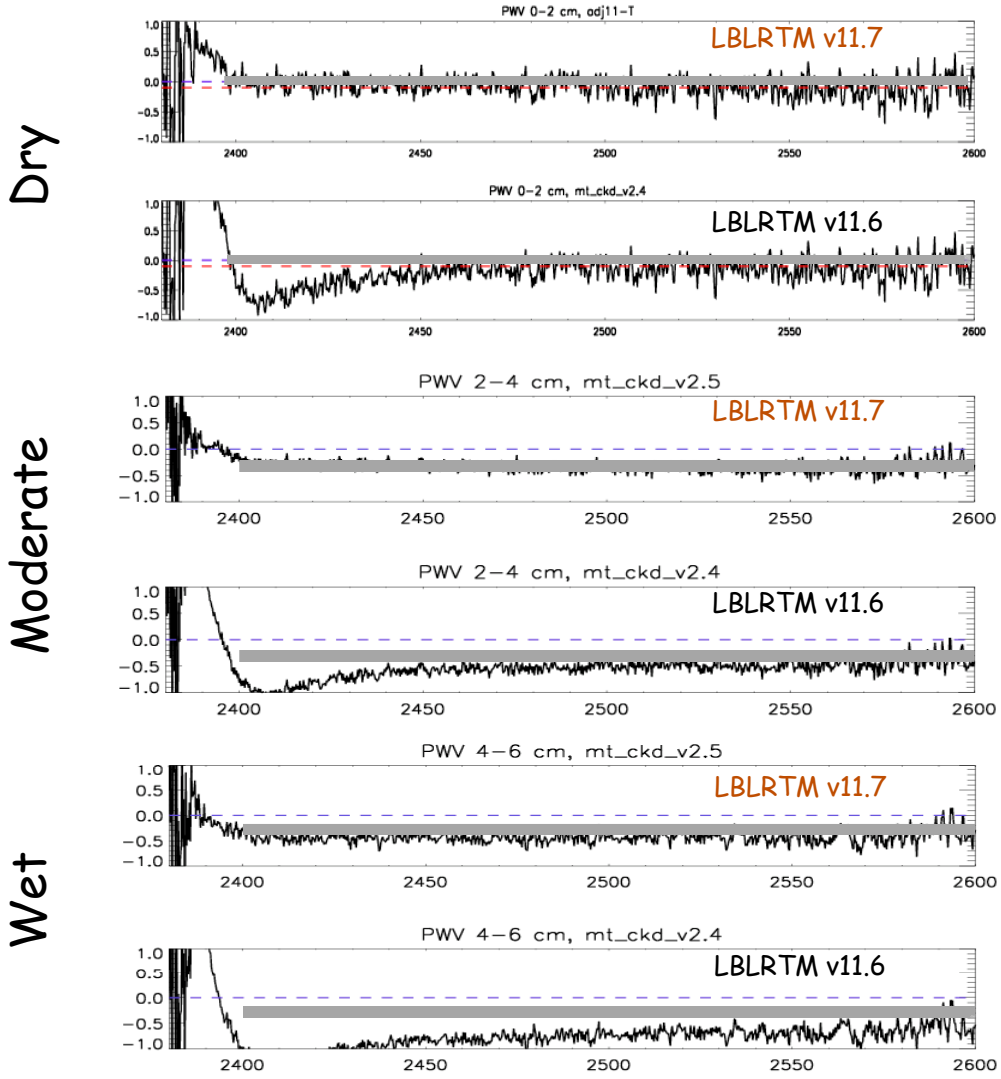

LBLRTM: future plans

- NLTE:
  - Added flexibility to accept user specified isotopes and NLTE bands (hard coded in current release) in special JCSDA release
- Future:
  - Test with larger set of IASI/RAOB match ups and adjust atmospheric profiles using the radiometric measurements in selected spectral regions
  - CO_2 667 cm^{-1} Q-branch (treatment of line coupling)
  - CH_4 line coupling
  - H_2O ν_2:
    - Line widths (R. Gamache, U. Mass Lowell)
    - Local continuum adjustment
    - HITRAN 2008 evaluation

MW Land surface property characterization

- Motivation:
  - Improve characterization of surface emissivity for atmospheric remote sensing
  - Provide estimates of LST under cloudy conditions (MW is only source of global remotely sensed LSTs under cloudy conditions)
- Applications:
  - Assimilation of MW sounder data over land
  - Improvement to cloud analysis
    - better LST provides potential for improving cloud characterization
  - LSM validation
  - Climate studies

Land retrieval problem

- Build upon NASA funded work to provide regularly updated surface emissivity maps (~40km resolution)
- AMSR-E emissivity retrieved using MODIS LST product in the clear-sky (and NCEP atmospheric field)
  - Good consistency between MODIS and AMSR measurements results in highly stable emissivities
- 11GHz polarization ratio used to monitor changes in physical surface characteristics during cloudy phases

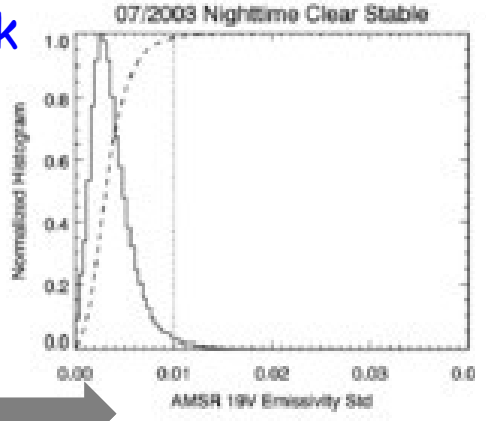

AMSR-E/MODIS derived product

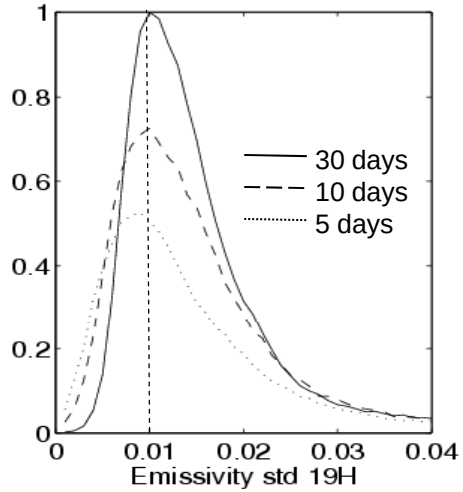

SSMI/ISCCP LST derived product (from Prigent)

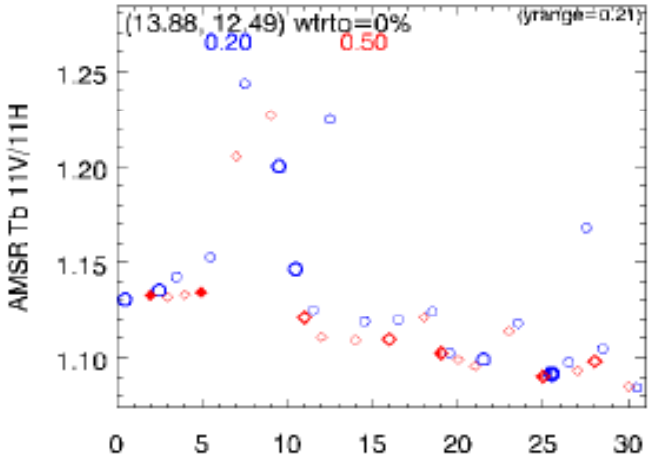

Impact of surface penetration

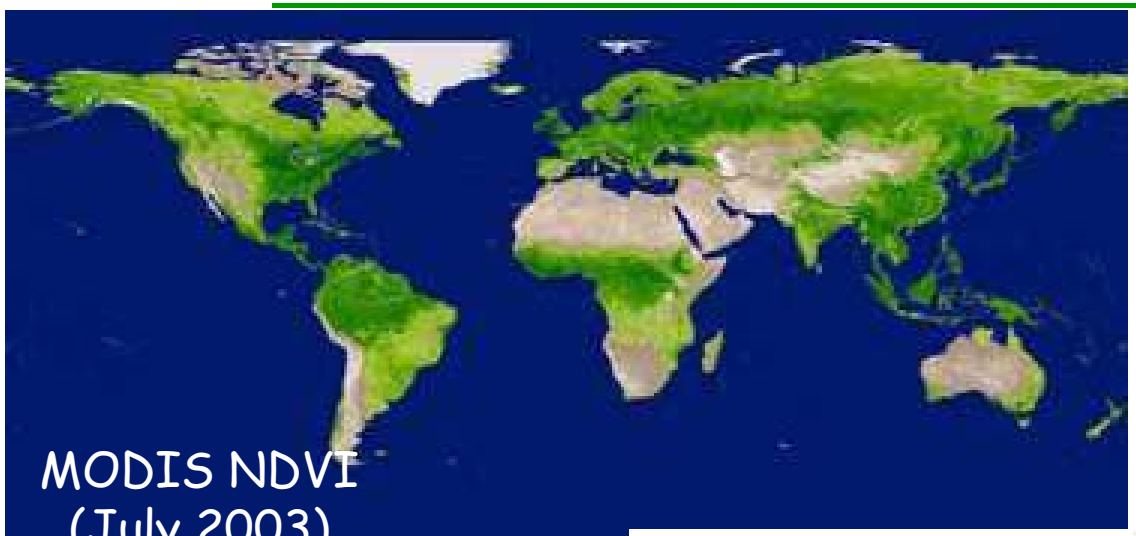

Subsurface temperature gradients at time of Aqua overpass give rise to strong day/night "swings" in retrieved emissivity when IR skin temperature is used as an estimate of MW emission temperature

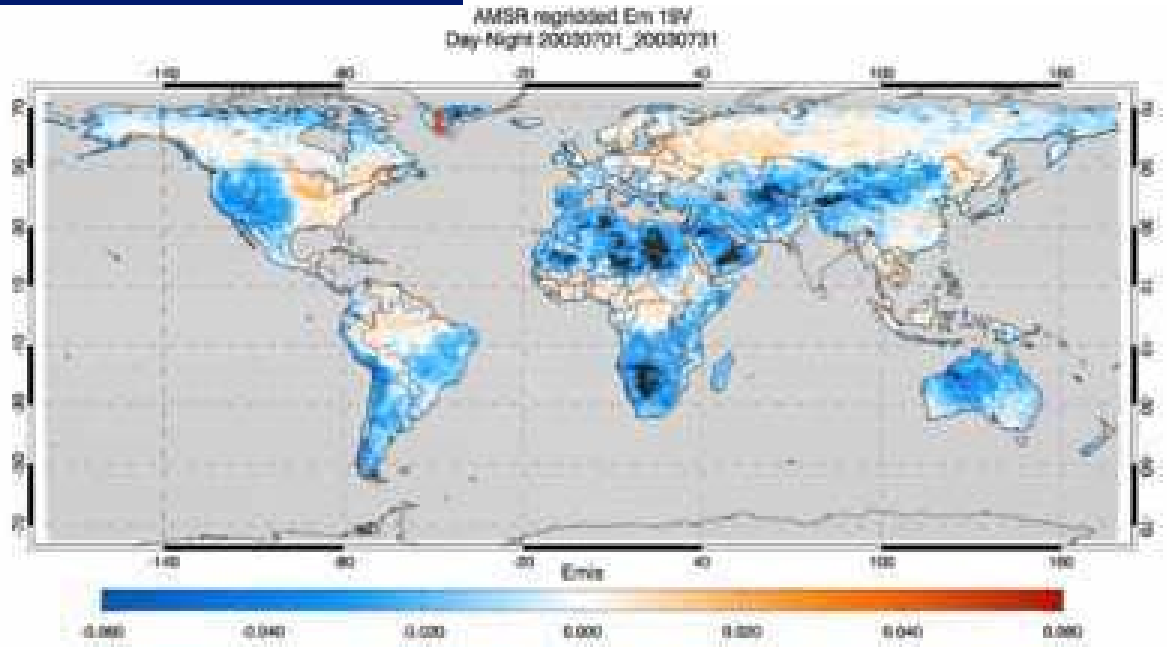

11V emissivity standard deviations (July 2003)

- 1a: applies to vegetated surface (penetration effects negligible) $T_{sfc\_MW} \sim T_{sfc\_IR}$
- C: substitute for 1a (from classification algorithm) in areas with persistent cloudiness
- 1b: emissivity derived from 1D thermal diffusion model using IR, AMSR and SSM/I measurements*

* Aqua/MODIS Tskin measurements currently used to set amplitude of the surface diurnal cycle (plan to include other IR sensors) 89 GHz Tb's from AMSR and SSM/I (sample different times of the day) provide phase reference

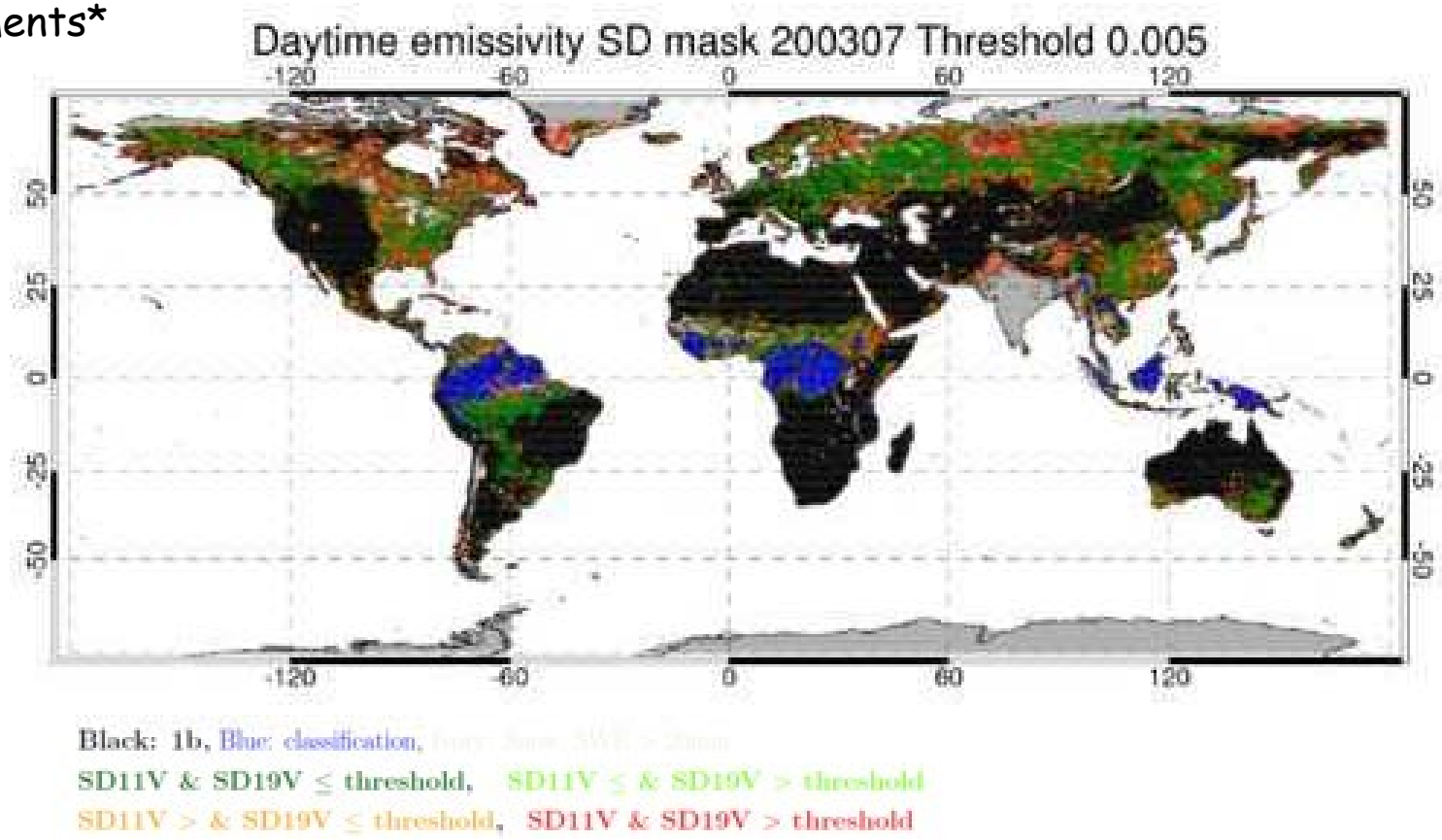

AMSR-E emissivities estimated using simple 1D thermal model

AMSR-E Database (emissivities more time-stable in arid and semi arid areas)

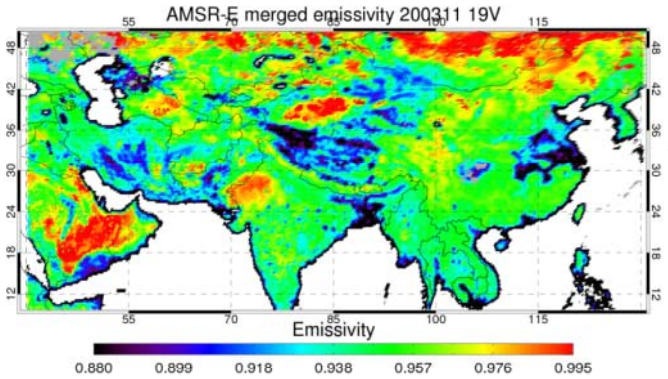

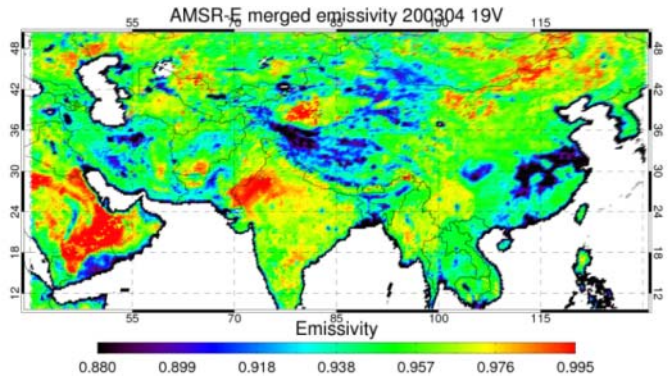

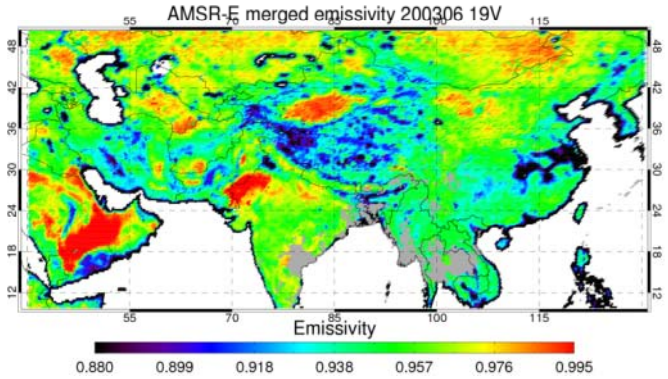

SSM/I Database

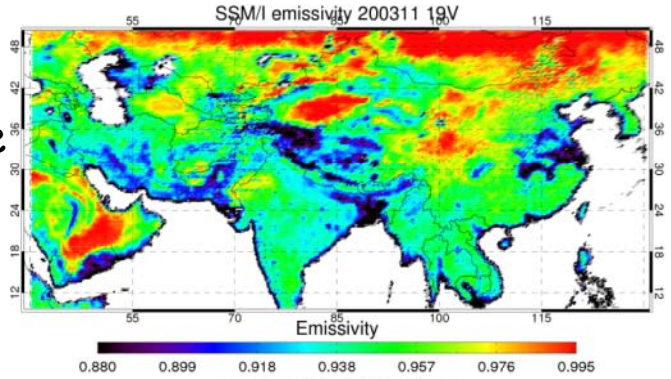

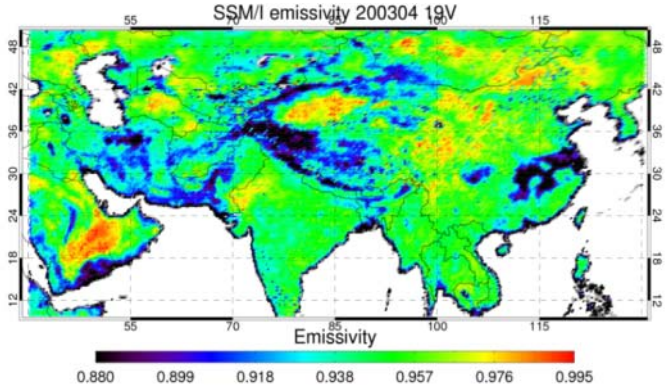

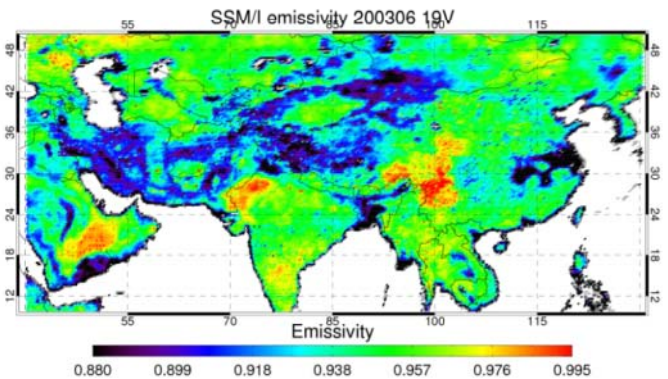

Validation sites

- FLUXNET
- ARM
- Special field campaigns: SMEX 05 and 09 (Hornbuckle et al., U. Iowa)

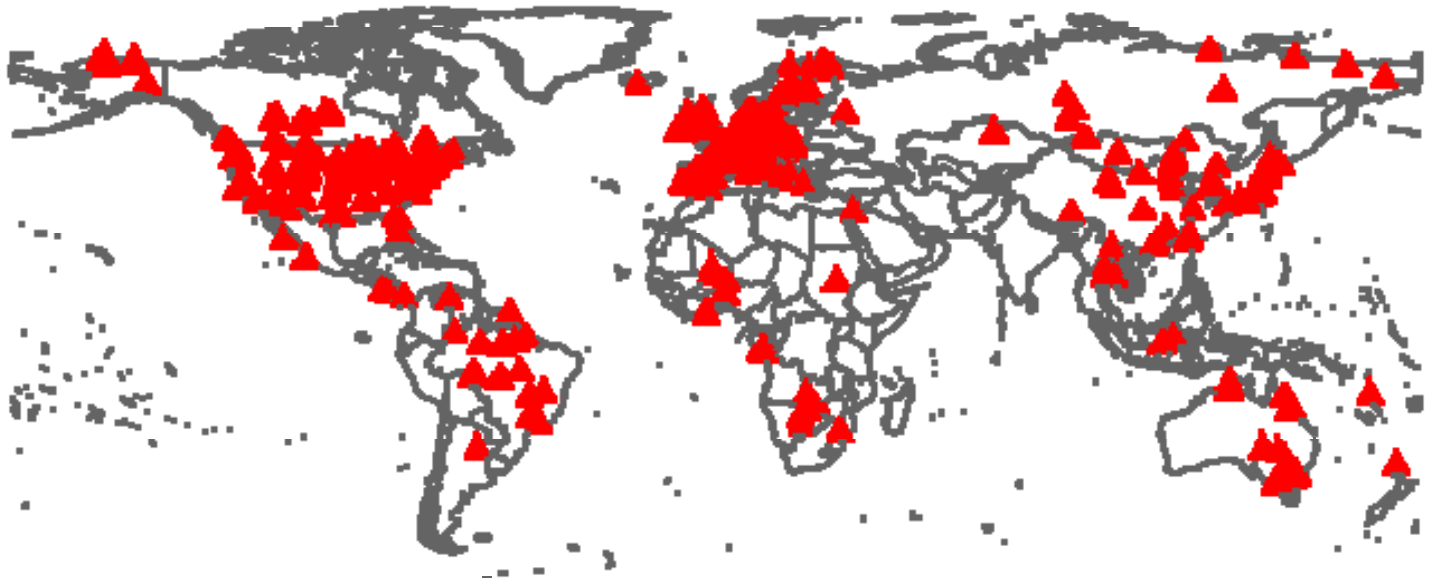

FLUXNET sites distribution map

Santarem FLUXNET site: LST/MW emissivity validation in the tropics

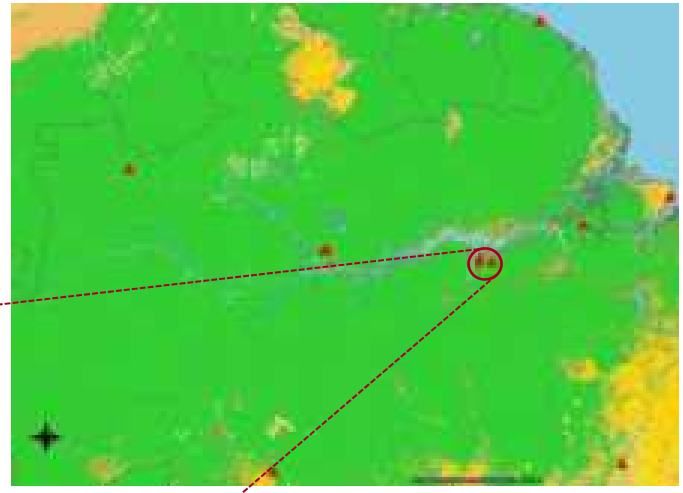

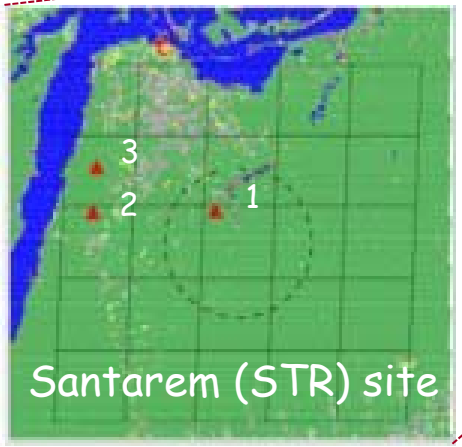

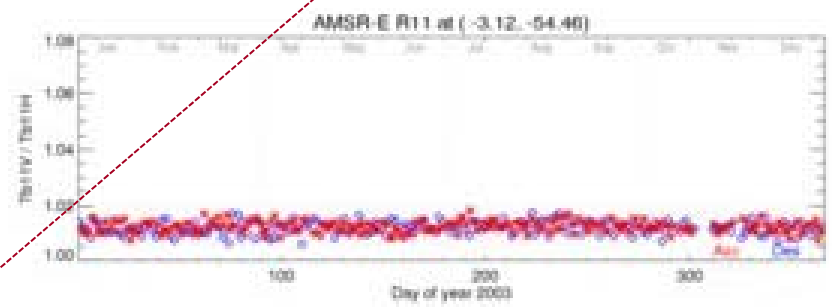

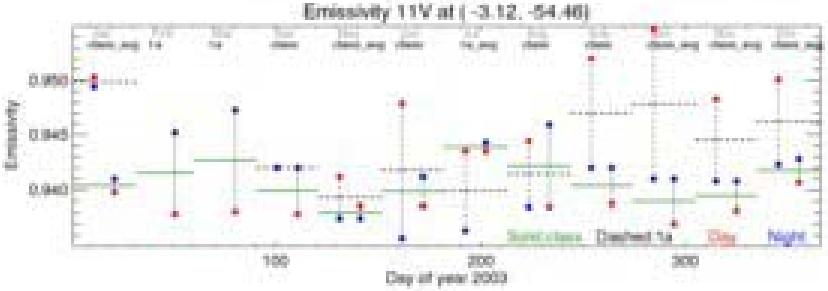

Example of validation results (no CLW correction)

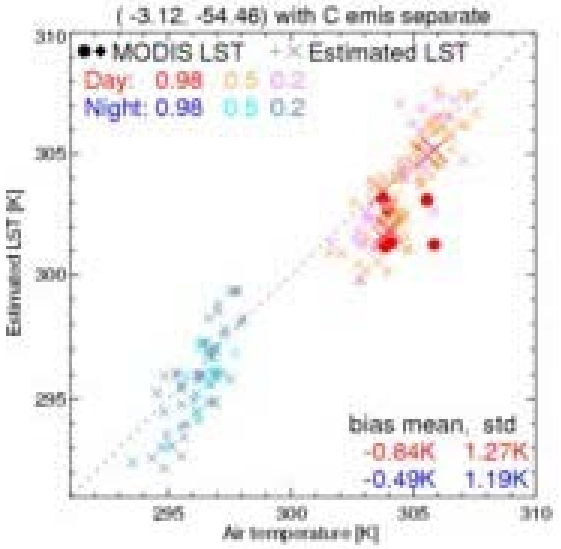

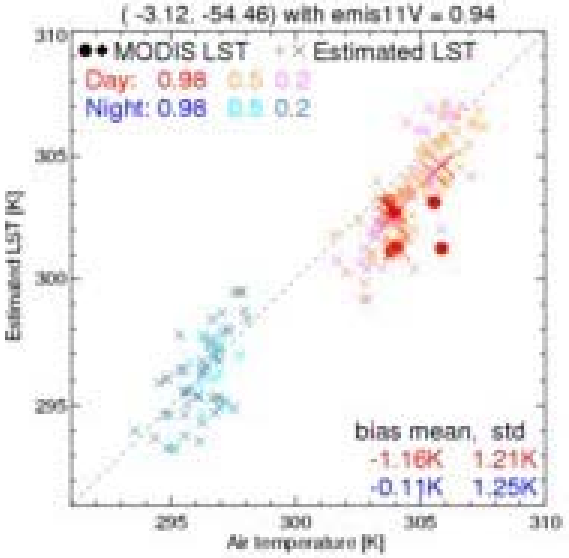

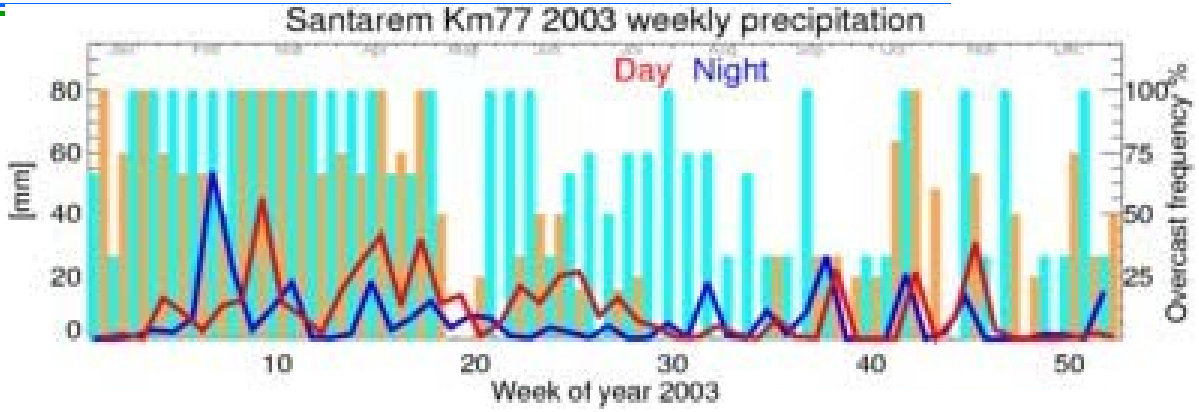

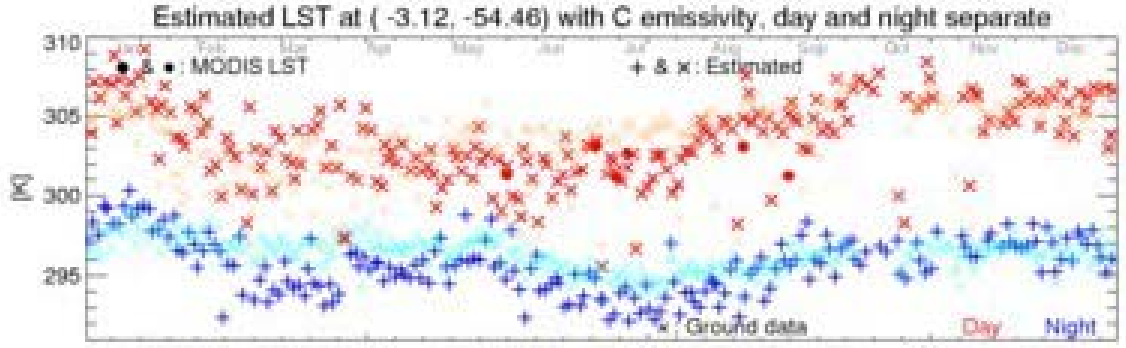

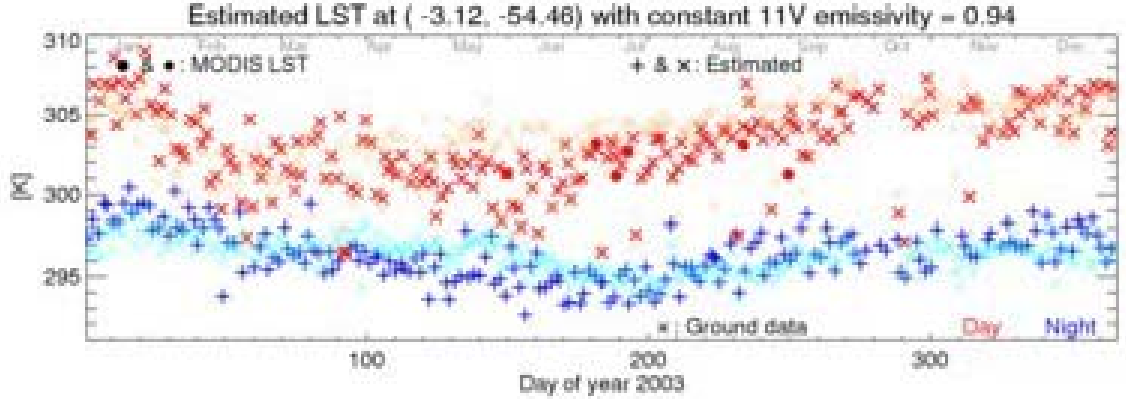

Validation results (continued)

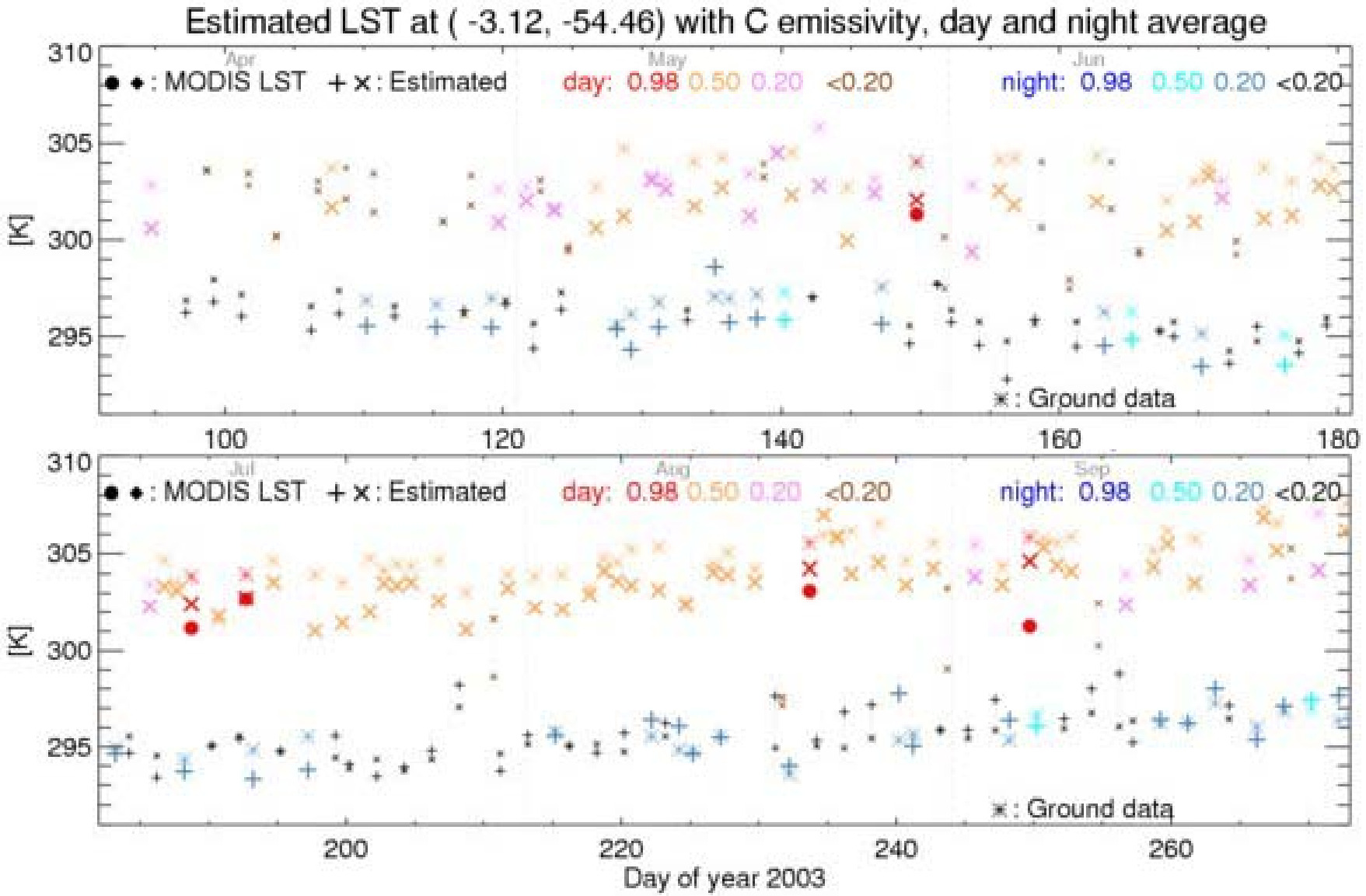

Positive day/night emissivity anomaly in the Midwest

- Systematic positive day/night differences in our AMSR-E/MODIS emissivity product are observed during the summer months in the Midwest
  - Spatial pattern appears to coincide with corn/soybean crop
  - Are these differences real or artifacts of our process/data?

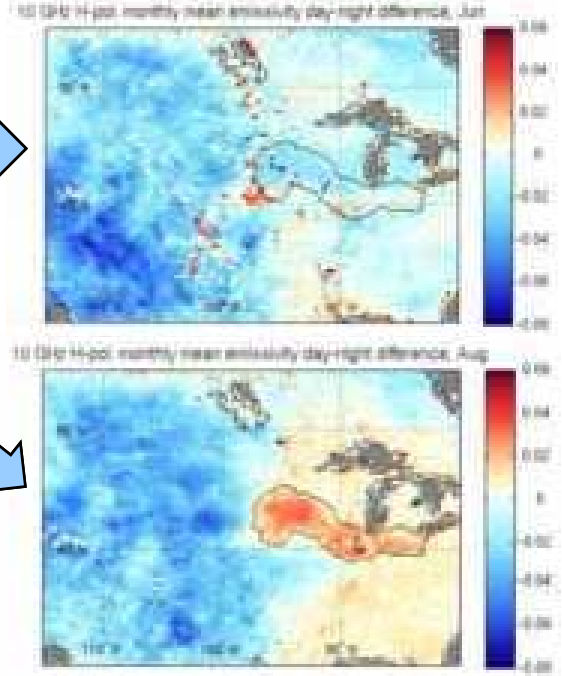

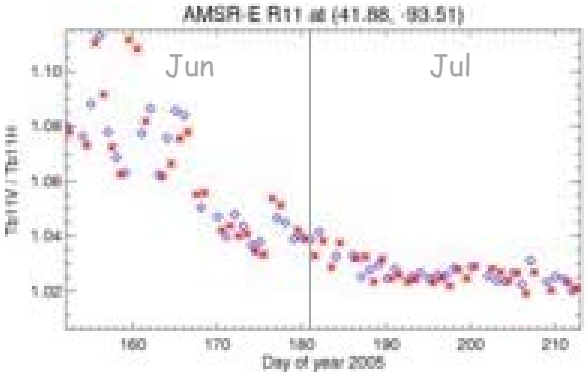

Monitoring corn growing season at 11 GHz

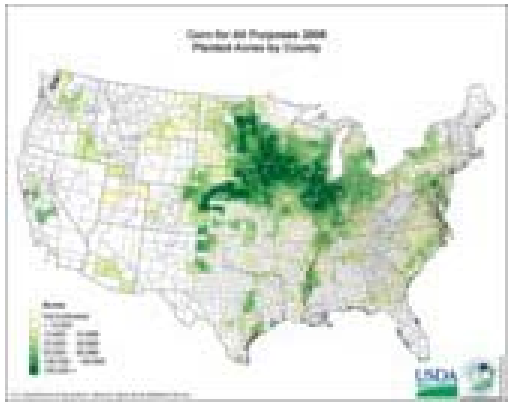

Comparison of ΔDN>0 & ΔDN≅0 regions

July-August, 2003

10 GHz ΔDN>0 (Iowa)

10 GHz ΔDN≅0 (Missouri)

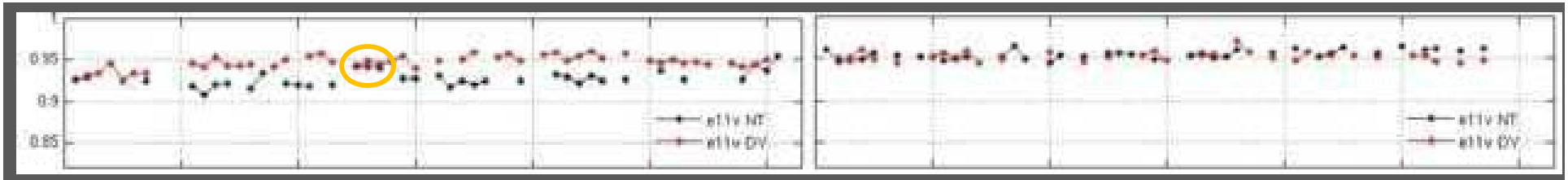

ε(day): 0.94 – 0.96 & e(night)<e(day) usually

ε(day) ≅ e(night): 0.94 – 0.96

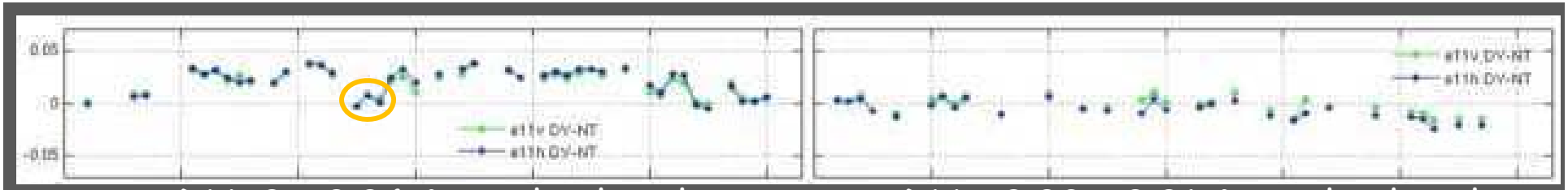

ΔDN: 0 – 0.04 & v-pol. ≅ h-pol.

ΔDN: -0.02 – 0.01 & v-pol. ≅ h-pol.

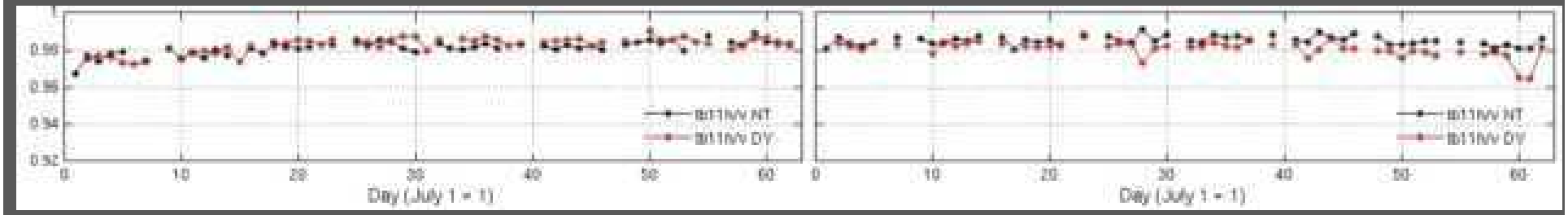

Polarization ratio (TB_H/TB_V): no large differences between regions

Evidence for emissivity reduction by dew on large-leaf crops (corn/soybean)

1. $\Delta DN > 0$ occurs most days in July-August
2. Nighttime dew at AMSR-E overpass time (~0130) is also persistent
3. $\Delta DN > 0$ region daytime emissivities are consistent with nearby $\Delta DN \cong 0$ regions
   - ε(night) occasionally rises to level of ε(day)
4. ΔDN is independent of polarization & there is little day-night polarization ratio difference
   - i.e., effect is quasi-polarization-neutral (not due to soil moisture)
5. Effect is strongly associated with mature, large-leaf crops (corn & soybeans)
   - Ground surface is obscured at 10 GHz
   - Large, dew-covered leaves may induce scatter-darkening (also seen at 1.4 GHz, Hornbuckle et al., 2007)

Preliminary analysis with 2009 (SMEX09) Iowa dew field measurements*

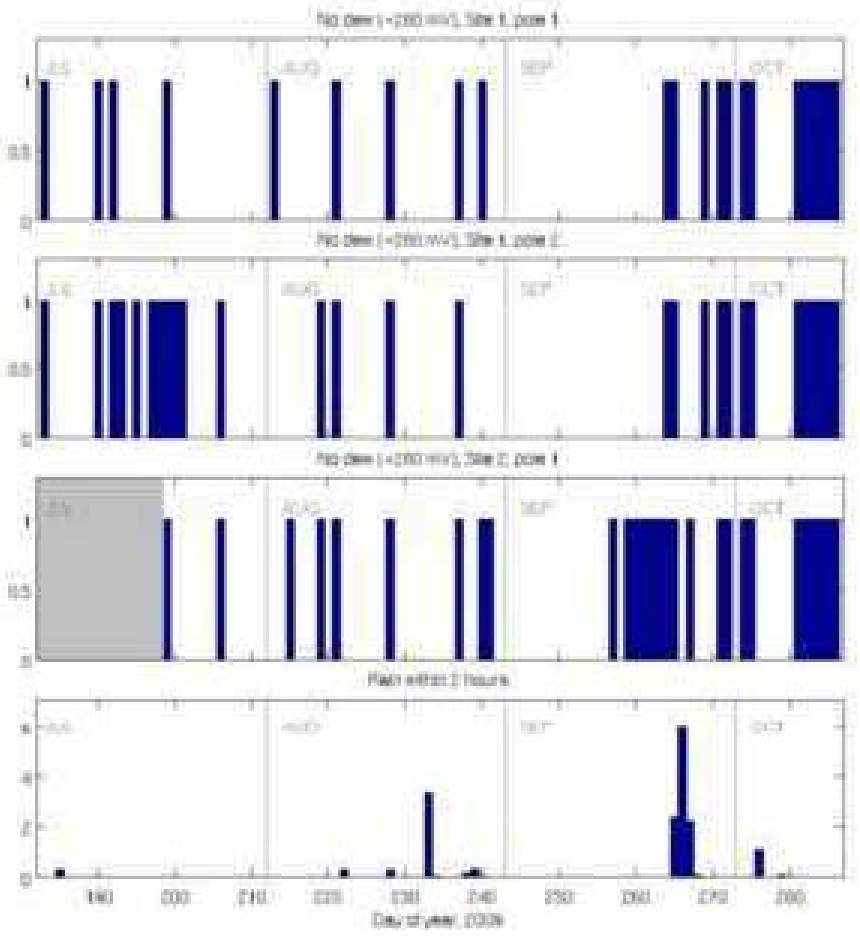

- Nighttime AMSR-E overpass times *without* detected dew
  - 3 automatic dew sensors (mV output)
- Sensor disagreement suggests light dew amount
- Ad hoc "no-dew" algorithm:
  - Any of 3 sensors reporting <280 mV

Reasonably good agreement between MODIS LST and in situ air temperatures in the clear-sky (night time)

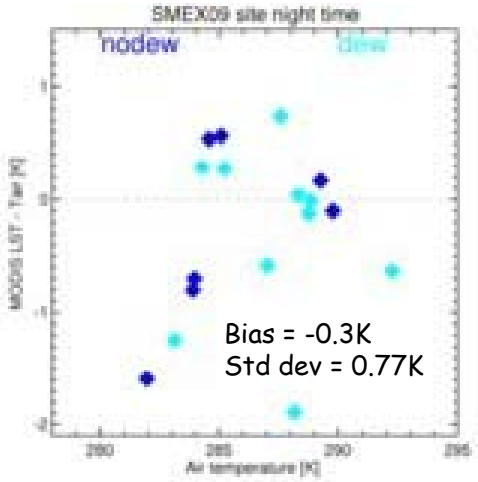

*Experiment conducted by Brian Hornbuckle from U. of Iowa

Results

- Preliminary analysis indicate correlation between ΔDN anomalies and occurrence of dew deposition on corn leaves

Night time emissivities
X: No dew X: Dew

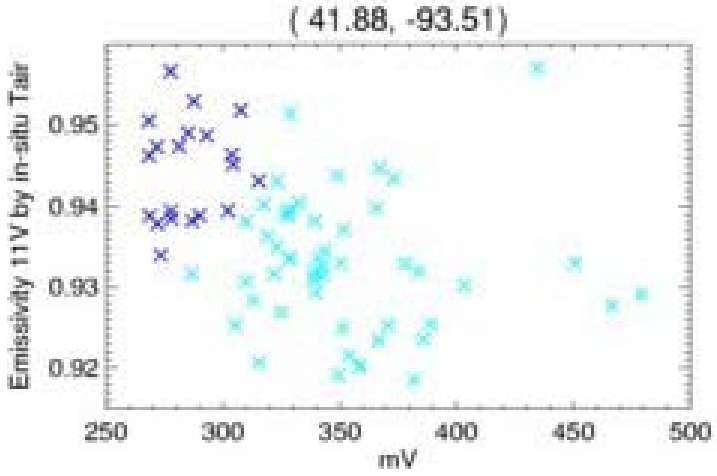

AMSR-E emissivities derived using in situ air temperatures at night

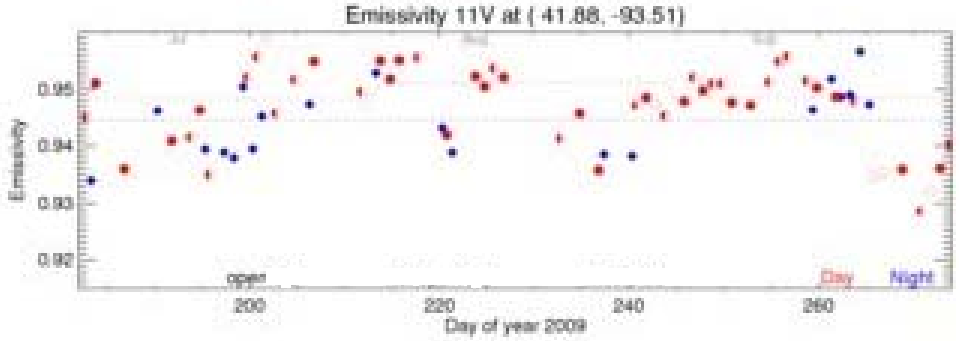

(a) No dew (see previous slide)

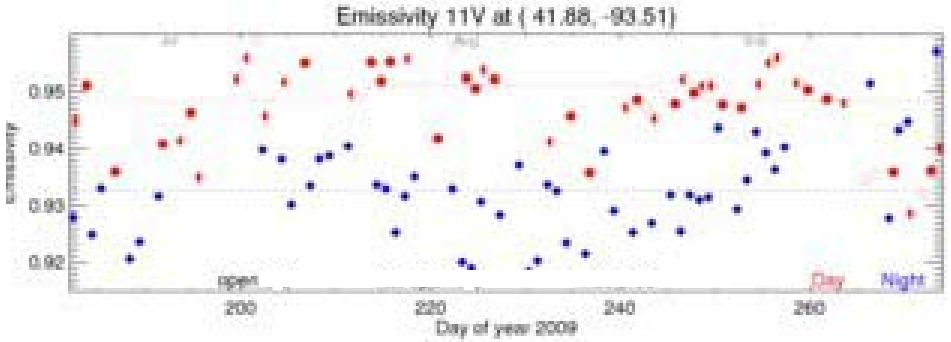

(b) Dew

Future plans

- OSS development
  - Refine generalized training and explore "node-based" compression as an alternative to EOF representation (and its impact on retrieval)
  - Build an OSS specific version of CRTM (?)
- LBLRT/MonoRTM
  - Continue validation and improvement (see slide 33)
- MW land emissivity database
  - Global monthly emissivities for yr 2003 delivered to JCSDA (includes spatially matched MODIS emissivities)
  - Continue validation over vegetated and arid regions and propose improvements
  - Produce global LST estimates (NASA/NEWS)

Future plans (continued)

- 4D-VAR Assimilation of cloud properties in WRF (AFWA/NCAR)

Comparison of 1DVar cirrus cloud retrieval product from MODIS with Calipso/CloudSat

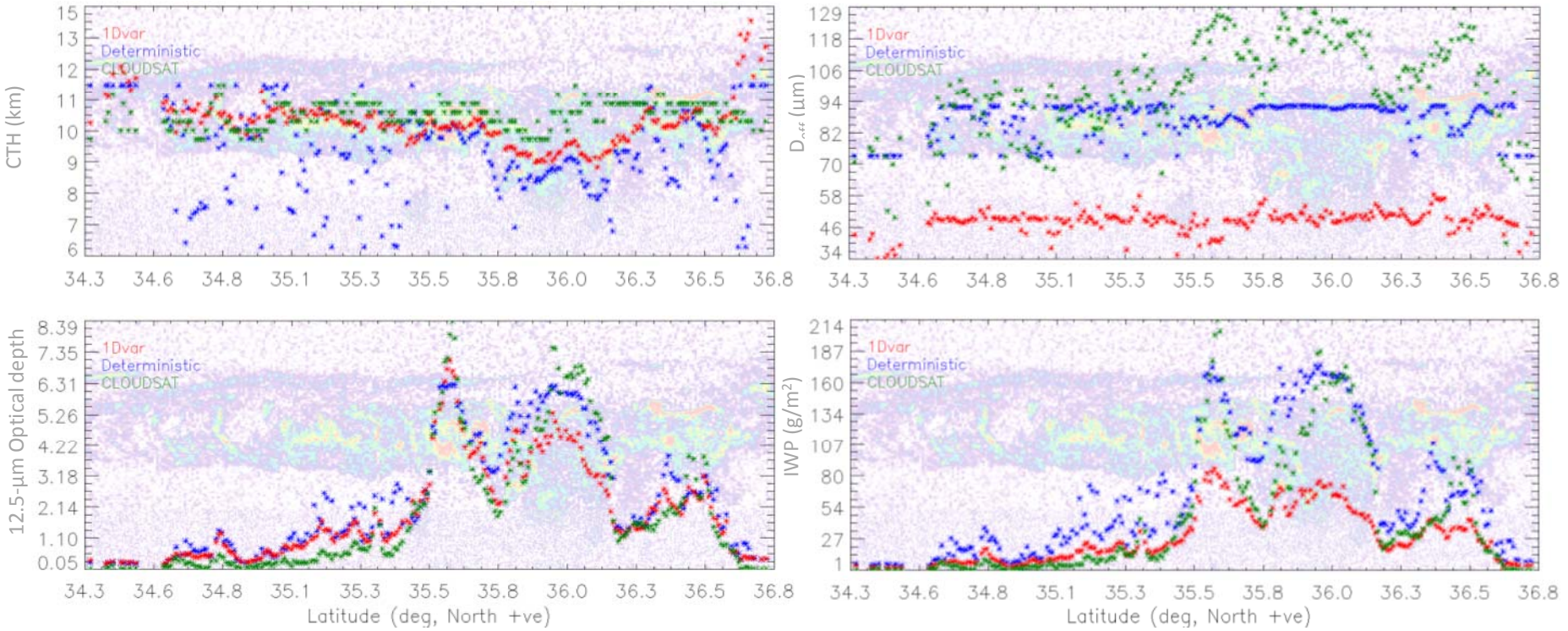

Calipso Backscatter (in background)